Mathematisches Forschungsinstitut Oberwolfach

Report No. 57/2009

DOI: 10.4171/OWR/2009/57

Material Theories

Organised by
Antonio DeSimone, Trieste
Stephan Luckhaus, Leipzig
Lev Truskinovsky, Palaiseau

December 13th – December 19th, 2009

Abstract. This biennial workshop brings together mathematicians, mechanicians and theoretical physicists interested in developing new mathematical models of complex materials, medias and systems. The workshop covers a wide range of topics from nonequilibrium statistical mechanics and dynamical systems to calculus of variations and nonlinear functional analysis. A particular focus of this meeting was on continuum description of biological systems, pattern formation, granular media, plasticity and turbulence.

Mathematics Subject Classification (2000): 35R60, 35K55, 35L65, 49J40, 49J45, 49Q20, 74B05, 74B20, 74K20, 74N20, 76B45, 76F55, 76M28, 78A70.

Introduction by the Organisers

The biennial workshop Material Theories organized by Antonio DeSimone, (Trieste), Stephan Luckhaus (Leipzig) and Lev Truskinovsky (Palaiseau) brings together mathematicians, mechanicians and theoretical physicists interested in developing new mathematical models of complex materials, medias and systems. The workshop covers a wide range of topics from nonequilibrium statistical mechanics and dynamical systems to calculus of variations and nonlinear functional analysis.

A particular focus of the 2009 meeting was on continuum description of biological systems, pattern formation, granular media, molecular dynamics, plasticity and turbulence. In addition to 25 general lectures the conference program included an evening talk on thermodynamic modeling of evolutionary genetics and an exceptional concert of classical music.

Among the highlights of the conference we would like to mention the talk of Florian Theil (Coventry), who presented a significant advance in 3D crystal problem,

the talk of Hans Herrmann (Zürich) devoted to the modeling of optimal fractal organization in moving granular systems and the talk of Yann Brenier (Nice) on multidimensional rearrangement theory and its relation to Navier-Stokes Boussinesq equations.

The exciting lectures of Jean-Francois Joanny (Paris), Frank Jülicher (Dresden), Karsten Kruse (Saarbrücken), Sebastien Neukirch (Paris), Paolo Cermelli (Torino) and Marta Lewicka (Minneapolis) reviewed new developments in the continuum representation of active biological systems (at both cellular and tissue level) which targeted such diverse applications as viruses, DNA, tumors and trees. Another novel and still poorly understood subject is pinning-depinning transition and the related self organized criticality. Mathematical progress in the related problems leading to power law spectrum of fluctuations was reviewed in the lectures of Luis Bonilla (Leganes) Nicolas Dirr (Bath), Francisco-Jose Perez-Reche(Cambridge) and Oguz Umut Salman (Palaiseau).

Borrowing most their tools from probability theory, Stefano Olla (Paris) and Sergei Kuksin (Palaiseau) discussed the averaged behavior of stochastically regularized nonlinear dynamical systems originating in the theory of heat conduction and fluid mechanics (nonequilibrium steady states). Recent progress in the classical problems of nonlinear solid mechanics, such as fracture, plasticity and strain localization was addressed in the lectures of Antonin Chambolle (Palaiseau), Davide Bigoni (Trento) and Luca Mugnai (Leipzig). More general issues of rate independent hysteresis, structural self-similarity, pattern formation and band gaps in continuum mechanical systems and the new mathematical tools developed for the adequate representation became the subject of the lectures of Giovanni Alberti (Pisa), Alexander Mielke (Berlin), Victor Berdichevsky (Detroit), Mark Peletier (Eindhoven) and Guy Bouchitte (La Garde). Recent advances in the rigorous study of coarse graining and the transition from discrete to continuum in both statics and dynamics were reviewed by Bernd Schmidt (München) and Antonio DiCarlo (Roma).

Overall, the workshop created an unprecedented opportunity for the researchers working in different disciplines to be exposed to new and fruitful ideas and to build otherwise impossible exchanges and collaborations.

Workshop: Material Theories

Table of Contents

Abstracts

Wetting and contact-angle hysteresis

Giovanni Alberti
(joint work with Antonio DeSimone)

Consider a drop E sitting on a solid surface S as shown in the picture below.

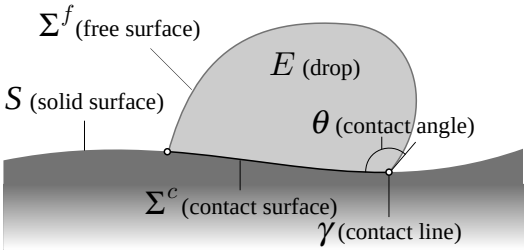

The classical model of capillarity (cf. [3]) postulates an energy of the form

$$\mathcal{E} = \sigma_{LV}|\Sigma^f| + \sigma_{LS}|\Sigma^c| + \sigma_{SV}|S \setminus \Sigma^c| + \text{volume energy}$$

where $|\Sigma|$ denotes the area of the surface Σ, the volume energy is usually given by the integral over E of an energy density ρ, and the coefficients σ_{LV}, σ_{LS}, σ_{SV} satisfy the wetting condition

$$|\sigma_{LS} - \sigma_{SV}| \leq \sigma_{LV}\,.$$

This energy yields the usual equilibrium conditions at fixed volume, namely Laplace's law

$$-2\sigma_{LV}H^f + \rho = \text{constant on } \Sigma^f\,,$$

where H^f stands for the mean curvature of the free-surface Σ^f (outward oriented) and the constant at the right-hand side corresponds to the pressure difference across the surface, and Young's law

$$\theta = \theta_Y \text{ on } \gamma\,,$$

where the angle θ_Y is defined by the relation

$$\cos\theta_Y := \frac{\sigma_{SV} - \sigma_{LS}}{\sigma_{LV}}\,.$$

Thus, according to this model, if E is an equilibrium configuration (e.g., a local minimizer of $\mathcal{E}$ at fixed volume) then the contact angle θ agrees with θ_Y at every point of the contact line γ.

Note that the following (observed) phenomena are not accounted for by this model:

1) A drop of water on an inclined plane may be in equilibrium, even though in presence of gravity the energy $\mathcal{E}$ would be decreased by sliding down, and in this case the contact angle is not constant.

2) If we increase the volume of a spherical drop on an horizontal plane, at first the contact line remains still while the contact angle increases until it reaches a

critical value $\theta_{\rm adv}$, and afterwards the contact angle remains constant $= \theta_{\rm adv}$ while the contact line advances (moves outward). Moreover, if at a certain moment we invert the process and start decreasing the volume, then at first the contact line remains still and the contact angle decreases until it reaches a critical value $\theta_{\rm rec}$, and afterwards the contact angle remains constant $= \theta_{\rm rec}$ and the contact line recedes. Thus we observe contact-angle hysteresis.

In order to account for these phenomena, following [2], in [1] we postulate that the contact line is subject to a frictional force described by the following condition: if the contact line γ moves with normal velocity v, the dissipation rate (energy dissipated per unit time) is

$$\mathcal{R} = \mu \int_\gamma |v| \, .$$

Indeed, if we define the angles $\theta_{\rm adv}$ and $\theta_{\rm rec}$ by the relations

$$\cos\theta_{\rm adv} := \cos\theta_Y - \frac{\mu}{\sigma_{LV}} \quad \text{and} \quad \cos\theta_{\rm rec} := \cos\theta_Y + \frac{\mu}{\sigma_{LV}}$$

(we assume that the parameter μ is such that the right-hand sides of these equations belongs to thew interval $[-1, 1]$), then the flow rules for the quasistatic evolution associated to this system – that is, to the energy $\mathcal{E}$ and the dissipation rate $\mathcal{R}$ – prescribe that at every time the free surface Σ^f satisfies Laplace's law, and the contact angle θ satisfies

- $\theta = \theta_{\rm adv}$ in the points of γ where $v > 0$;
- $\theta = \theta_{\rm rec}$ in the points of γ where $v < 0$;
- $\theta_{\rm rec} \le \theta \le \theta_{\rm adv}$ in the points of γ where $v = 0$.

Therefore these flow rules explain the contact-angle hysteresis described above.

On the analysis side, following the work of A. Mielke and coauthors (see [5] for a detailed overview, a similar approach was proposed in [4]) we prove the existence in a suitable weak setting of quasistatic evolutions with given initial configuration (what drives the evolution is the volume of the drop, which varies in time in a prescribed way, and possibly the volume forces). More precisely, we show that a quasistatic evolution can be obtained by taking the limit in time-discretized evolutions as the time-discretization parameter tends to 0.

An interesting feature of this relatively simple geometric model is that in some cases quasistatic evolutions can be explicitly written, and, not surprisingly, it turns out that they may be discontinuous in time (the drop jumps instantly from one configuration to another). In one of these examples the predicted behaviour at the discontinuity is clearly unphysical, and this suggests that our notion of quasistatic evolution should be refined, e.g. by adding a suitable vanishing viscosity.

References

[1] G. Alberti, A. DeSimone, *Quasistatic evolution of sessile drops and contact angle hysteresis*, paper in preparation.

[2] A. DeSimone, N. Gruenewald, F.Otto, *A new model for contact angle hysteresis*, Network and Heterogeneous Media **2** (2007), 211-225.

[3] R. Finn, *Equilibrium Capillary Surfaces*, Grundlehren der Mathematischen Wissenschaften, 284. Springer-Verlag, New York, 1986.
[4] G. Francfort, J.-J. Marigo, *Revisiting brittle fracture as an energy minimization problem*, J. Mech. Phys. Solids **46** (1998), 1319–1342.
[5] A. Mielke, *Differential, energetic, and metric formulations for rate independent processes*, preprint no. 1454, Weierstrass Institute for Applied Analysis and Stochastic, Berlin, 2009.

Statistical origin of microstructure self-similarity in severe plastic deformation

Victor L. Berdichevsky

One of the most remarkable experimental findings of recent years in material science was the discovery of self-similarity of microstructures in severe plastic deformations of polycrystals. It was made by Hughes et al. [2], [3] and further developed in a series of publications by Hansen, Hughes and their coauthors. They studied the microstructure of cold rolled aluminum, copper and nickel in case of large shear deformation, up to a von Mises strain 6. In such highly sheared materials the microstructure is predominantly laminar. The laminar microstructure exhibits the "turbulent" features: the misorientation angle of crystal lattices in neighboring laminae, θ, and lamina thickness, a, are random. The probability density functions of a and θ were found by working out the experimental data. It turned out that the random numbers, a and θ, after being scaled by their average values, $\bar{a}$ and $\bar{\theta}$, have the universal distributions that are independent on strains and materials tested.

In this talk a simple statistical model is suggested, which admits an analytical investigation and yields the distributions of $a/\bar{a}$ and $\theta/\bar{\theta}$. The model is based on the following schematic picture of the microstructure.

Consider a crystal which is clamped at one side, while the opposite side is sheared and/or compressed by a prescribed displacement. The displacement is of the order of the length of the piece, L. Thus, a finite plastic strain develops. The plastic deformation is accompanied by the formation of a laminar microstructure. The microstructure consists of N laminae with the thicknesses $a_1, a_2, ..., a_N$. The plastic deformation of each lamina occurs due to nucleation and multiplication of dislocations. Dislocations sitting in a lamina cause the change of the crystal orientation of this lamina as compared to the orientation of the perfect lattice. The absolute value of the misorientation of kth layer is denoted by α_k. The absolute value of the crystal lattice misorientation is neighboring layers is set equal to the sum,

$$\theta_k = \alpha_{k-1} + \alpha_k. \tag{1}$$

So, the microstructure is characterized by the set of $2N$ positive numbers, $a_1, a_2, ..., a_N$ and $\alpha_1, \alpha_2, ..., \alpha_N$. To describe the statistics of these numbers, we have to define the probability of elementary events. As such we will use the probability measure suggested in [1]: the microstructures with the same value of energy

are equiprobable. It is assumed, of course, that the admissible parameters must satisfy the kinematic constraints, like, e.g., the sum of all lamina thicknesses must be equal to the length of the specimen, L,

$$a_1 + a_2 + ... + a_N = L. \tag{2}$$

We make two major assumptions. First, the energy of the microstructure, H, is a linear function of α_k :

$$H = 2\gamma_0 (\alpha_1 + ... + \alpha_N) |\Omega| . \tag{3}$$

Here $|\Omega|$ is the area of the specimen cross-section $x = const$, γ_0 a constant.

Second, the parameters α_i and a_i are not kinematically independent. A certain number of dislocations is needed to create a grain boundary. The number of dislocations generated in the kth lamina is proportional to the misorientation of the lamina α_k. For zero α_k, no grain boundary is generated, or, in other words, the grain boundary spacing is infinite. For small α_k, the grain boundary spacing must be large. The larger α_k, the smaller a_k. We accept that there is "microstructure quantum number", $\varkappa$, such that the product of α and a for all grains is the same:

$$\alpha_1 a_1 = \alpha_2 a_2 = ... = \alpha_N a_N = \varkappa. \tag{4}$$

The constant $\varkappa$ has the dimension of length.

The relation (4) makes $\alpha_1, ..., \alpha_N$ certain functions of the spacings and eliminates them from the set of the independent characteristics of the microstructure. Energy becomes a function of spacings,

$$H = 2\gamma_0 \varkappa |\Omega| \left(\frac{1}{a_1} + ... + \frac{1}{a_N} \right). \tag{5}$$

Formulas (2)-(4) define the probabilistic measure: all microstructures which lie in the region

$$E \leqslant 2\gamma_0 \varkappa |\Omega| \left(\frac{1}{a_1} + ... + \frac{1}{a_N} \right) \leqslant E + \Delta E$$

$$L \leqslant a_1 + ... + a_N \leqslant L + \Delta L$$

are equally probable. This yields the probability density function of spacings,

$$f(a_1, .., a_N) = c\delta (E - H(a_1, .., a_N)) \delta (L - a_1 - ... - a_N), \tag{6}$$

where c is a normalizing constant.

Computation of probability density function of thicknesses of the first layer, a_1, is reduced to computation of the integral,

$$f(a) = \int f(a, a_2, .., a_N) da_2 ... da_N. \tag{7}$$

The probability density of misorientation angles is determined from (1) and (4). The probability densities are computed in the thermodynamic limit when $N \to \infty$ while energy per one layer, E/N, and average thickness, L/N, remain finite. The probability densities exhibits the proper scaling by average values $\bar{a}$ and $\bar{\theta}$ and coincide reasonably well with the experimental data.

References

[1] V.L. Berdichevsky, *Entropy of microstructure*, J. of Mech.and Phys. of Solids **56** (2008), 742–771.

[2] D.A. Hughes, Q. Liu, D.C. Chrzan, and N. Hansen, *Scaling of microstructural parameters: misorientations of deformation induced boundaries*, Acta Mater. **45** (1997), 105–112.

[3] D.A. Hughes, N. Hansen, *High angle boundaries formed by grain subdivision mechanisms*, Acta Mater. **45**. 3871–3886.

Material instabilities and the perturbative approach in solid mechanics

Davide Bigoni

Localized deformations in the form of shear bands emerging from a slowly varying deformation field are known to be the preferential near-failure deformation modes of ductile materials. Therefore, shear band formation is the key concept to explain failure in many materials and, according to its theoretical and practical importance, it has been the focus of an enormous research effort in the last 30 years. From the theoretical point of view, this effort has been mainly directed in two ways, namely the dissection of the specific constitutive features responsible for strain localization in different materials and the struggle for the overcoming of difficulties connected with numerical approaches.

Although these problems still seem far from being definitely solved, the most important questions in this research area have only marginally been approached and are therefore still awaiting explanation. They are as follows.

(i) The highly inhomogeneous stress/deformation state developing near a shear band tip is unknown from an analytical point of view (and numerical techniques can hardly have the appropriate resolution to detail this).

(ii) It is not known if a shear band tip involves a strong stress concentration.

(iii) The fact that shear bands grow quasi-statically and rectilinearly for remarkably long distances under mode II loading conditions, while the same feature is not observed in the akin problem of crack growth, remains unexplained.

(iv) Finally, and most importantly, the reason why shear bands are preferential failure modes for quasi-statically deformed ductile materials has no justification.

Answers to the questions above are provided employing the perturbative approach proposed by Bigoni and Capuani in [1], [2] and Piccolroaz et al. in [7], as extended to perturbing agents in terms of rigid line inclusions and slip surfaces (see [3], [5], [4], [6]).

References

[1] D. Bigoni, and D. Capuani, *Green's function for incremental nonlinear elasticity: shear bands and boundary integral formulation*, J. Mech. Phys. Solids **50** (2002), 471–500.

[2] D. Bigoni, and D. Capuani, *Time-harmonic Green's function and boundary integral formulation for incremental nonlinear elasticity: dynamics of wave patterns and shear bands*, J. Mech. Phys. Solids **53** (2005), 1163–1187.

[3] D. Bigoni, and F. Dal Corso, *The unrestrainable growth of a shear band in a prestressed material*, Proc. Royal Soc. A **464** (2008), 2365–2390.

[4] D. Bigoni, F. Dal Corso, and M. Gei, *The stress concentration near a rigid line inclusion in a prestressed, elastic material. Part II Implications on shear band nucleation, growth and energy release rate*, J. Mech. Phys. Solids **56** (2008), 839–857.
[5] F. Dal Corso, and D. Bigoni, *The interactions between shear bands and rigid lamellar inclusions in a ductile metal matrix*, Proc. Royal Soc. A **465** (2009), 143–163.
[6] F. Dal Corso, D. Bigoni, and M. Gei, *The stress concentration near a rigid line inclusion in a prestressed, elastic material. Part I Full-field solution and asymptotics* J. Mech. Phys. Solids **56** (2008), 815–838.
[7] A. Piccolroaz, D. Bigoni, and J.R. Willis, *A dynamical interpretation of flutter instability in a continuous medium*, J. Mech. Phys. Solids **54** (2006), 2391–2417.

Waves in nonlinear discrete systems

Luis L. Bonilla
(joint work with Ana Carpio, Holger Grahn, Guido Dell'Acqua, Ignacio Arana)

The damped Frenkel-Kontorova model of dislocations [1, 2], the spatially discrete FitzHugh-Nagumo (FHN) model of nerve conduction in myelinated neurons [3] or the discrete drift-diffusion model of electron transport in doped semiconductor superlattices (SL) [4] are examples of nonlinear discrete systems. These models are described by systems of coupled autonomous differential-difference equations having nonlinear N-shaped source terms and their dynamical behavior can be understood in terms of fronts, pulses or wave trains.

Wave fronts have monotone profiles joining two different constant solutions as the discrete index i goes to $-\infty$ or $+\infty$. These fronts are either traveling wave solutions moving at a constant velocity or stationary solutions (in whose case we say that the fronts are pinned by the lattice). Typically stationary fronts exist when a control parameter (the load in the FK model or the current J in the superlattice model) takes values on an open interval. The transition between moving and pinned fronts (pinning-depinning transition) depends on the dynamics of the system. For the overdamped FK model or the SL model, it is a global saddle-node bifurcation such that the front velocity vanishes as $c(J) \propto |J - J_c|^{1/2}$ as J goes to one of the extremes of the pinning interval [4, 5]. To be precise, consider the SL case:

$$\frac{dE_i}{dt} + v(E_i)\,\frac{E_i - E_{i-1}}{\nu} - D(E_i)\,\frac{E_{i+1} + E_{i-1} - 2E_i}{\nu} = J - v(E_i), \tag{1}$$

in which the pinning interval is (J_{c1}, J_{c2}). $E_i(t)$ are electric field values at the SL quantum wells, $v(E)$ and $D(E)$ are the electron drift velocity and diffusivity, respectively [4]. The critical currents J_{c1} and J_{c2} depend on another parameter, the dimensionless doping density ν. For $J > J_{c2}$, the wave fronts move towards the left, with negative velocity, whereas they move to the right if $J < J_{c1}$. As $J \to J_{c1}-$ or $J \to J_{c2}+$, the front profile develops steps (and it loses smoothness at the critical currents). For large values of ν there is one prominent step in the front profile: most $E_i(t) = E(i - ct)$ are either $E^{(1)}(J)$ or $E^{(3)}(J)$, with $v(E^{(n)}(J)) = J$, except for a single *active* point $E_0(t)$ which is in between these two values. The evolution of $E_0(t)$ is given approximately by (1) with $E_i =$

$E^{(1)}(J)$ for $i < 0$ and $E_i = E^{(3)}(J)$ for $i > 0$. The front profile $E(z)$ can be reconstructed from the motion of the active point by using $E(z) = E_0(-z/c)$ [1, 4, 5]. For J in the pinning interval, the equation for E_0 has one unstable and two stable stationary solutions. The unstable and one of the stable solutions merge in a saddle-node bifurcation as $J \to J_{cn}$, $n = 1, 2$. As $J \to J_{c1}-$ or $J \to J_{c2}+$, the corresponding normal form $d\varphi/dt = \alpha(J - J_{cn}) + \beta^2\varphi^2$, has the solution $\varphi = (-1)^n\sqrt{\alpha(J - J_{cn})/\beta}\,\tan[\sqrt{\alpha\beta(J - J_{cn})}\,(t - t_0)]$, which blows up at $(t - t_0) = \pm 1/(2c)$, with $c = \sqrt{\alpha\beta(J - J_{cn})}/\pi$. c is the approximate front velocity. At the blow-up times, $E_0(t)$ solves (1) with $J = J_{cn}$, $E_i = E^{(1)}(J)$ for $i < 0$ and $E_i = E^{(3)}(J)$ for $i > 0$, and the matching conditions $E_0 \to E^{(3)}(J_{cn})$ as $(t - t_0) \to +\infty$ for $(t - t_0) = 1/(2c)$ (resp. $E_0 \to E^{(1)}(J_{cn})$ as $(t - t_0) \to -\infty$ for $(t - t_0) = -1/(2c)$). As ν decreases, there are more active points between $E^{(1)}(J)$ and $E^{(3)}(J)$ and finitely many equations need to be kept to approximate (1). See Ref. [5] for a detailed description and results. In the continuum limit, $\nu \to 0$, the pinning interval disappears and (1) may be approximated by a first-order hyperbolic equation together with shock and entropy conditions that yield approximate wave front velocities [4].

The pinning-depinning transition of wave fronts is modified by disorder. For example, fluctuations in the SL doping density result in adding a term $\gamma D(E_i)(\xi_{i+1} - \xi_i) - \gamma v(E_i)\xi_i$ to the right hand side of (1), where ξ_i is a random variable taking values on $(-1, 1)$ with equal probability and $\gamma \to 0$. An extension of the active point theory has been used to show that the effect of disorder is to shift the critical currents and to change the critical exponent from 1/2 to 3/2 [6]. The effect of inertia may be even more dramatic. In the underdampled FK model with a piecewise linear source, the pinning-depinning transition may become subcritical: the stable branch of moving fronts is connected to the stationary solution by branches having infinitely many turning points that accumulate at the static critical J [2].

Wave fronts are stable solutions of the differential-difference equations considered here. We can use their profiles and velocities to describe more complex dynamical behaviors. Two examples. A voltage biased SL is described by (1) for $i = 1, \ldots, N$, the bias condition $\sum_{i=0}^{N} E_i = (N + 1)\,\phi$ (for a given constant voltage ϕ) and boundary conditions at $i = 0$ and N. The unknowns in this problem are $E_i(t)$ and $J(t)$. Depending on the values of ν and ϕ, this problem has stable stationary or time-periodic solutions which can be visualized in a bifurcation diagram of J versus ϕ (current-voltage diagram) [7]. For large ν, the only stable solutions are stationary and there may be several stable solution branches for a given value of ϕ. The field profile of each solution branch is a stationary wave front pinned at a given SL period i. For lower doping densities, there are intervals of ϕ for which the stable solutions are self-sustained oscillations having a periodic $J(t)$. The corresponding field profiles are pulses moving from $i = 0$ to $i = N$. These pulses are regions with $E_i = E^{(3)}(J)$ bounded by monotonically increasing and monotonically decreasing wave fronts. Between pulses or between pulses and contacts, $E_i = E^{(1)}(J)$. During a self-oscillation, $J(t)$ varies slowly whereas the field (either at wave fronts or at flat regions with

$E_i = E^{(n)}(J)$) adapts rapidly to the instantaneous value of J. To find an equation for $J(t)$, we simply time-differentiate the voltage bias condition, use the known functions $c_\pm(J)$ (velocities of a monotone increasing or decreasing wave front in terms of J) and that $v'(E^{(n)}(J))\, dE^{(n)}/dt = dJ/dt$. The result is an equation $dJ/dt = A(J)\,[n_+c_+(J) - n_-c_-(J)]/N$, where $n_\pm$ is the number of increasing (+) or decreasing (-) fronts and $A(J,\phi) > 0$ is a known function. If we include stages of wave front formation and annihilation at contacts, this equation is the basis of an asymptotic description of self-oscillations in the limit of large N (long SL) [7].

The other example of reducing pulse dynamics to wave front dynamics is provided by the FHN system consisting of an overdamped FK equation for the excitatory unknown and a linear ODE for the recovery unknown (the load). Their respective time scales are widely separated. In the fast time scale, the recovery variable is frozen and there are monotone increasing and decreasing fronts bounding a pulse of the excitatory variable. In the slow time scale, the excitatory variable moves over the stable branches of the N-shaped source term for the overdamped FK equation following the evolution of the recovery variable. It is possible to find a reduced system of equations for the time lag between wave fronts, the length of the region between fronts and the values of the recovery variable at the fronts [3]. The solution of this reduced system describe the evolution of the pulse.

Recently, we have considered a model for electron and hole transport in an undoped SL. In addition to a discrete drift-diffusion equation similar to (1), this system has an additional equation for the hole density plus bias and boundary conditions. If the electron-hole recombination is calculated as a function of electric field, the resulting system may have excitable or oscillatory dynamics with only one stable constant stationary solution, a situation reminiscent of the FHN system [8]. The voltage bias condition gives rise to a large variety of oscillations mediated by wave fronts, pulses and wave trains. Different from the case of doped SL, a pulse may be created inside the SL (not at the contact region), split into two, and each resulting pulse then moves towards the closest contact. Repetition of this process produces chaotic current oscillations.

References

[1] A. Carpio, L.L. Bonilla, *Wave front depinning transition in discrete one-dimensional reaction-diffusion systems*, Physical Review Letters **86** (2001), 6034–6037.

[2] A. Carpio, L.L. Bonilla, *Oscillatory wave fronts in chains of coupled nonlinear oscillators*, Physical Review E **67** (2003), 056621-1–056621-11.

[3] A. Carpio, L.L. Bonilla, *Pulse propagation in discrete systems of coupled excitable cells*, SIAM J. Appl. Math. **63** (2003), 619–635.

[4] A. Carpio, L.L. Bonilla, G. Dell'Acqua, *Motion of wave fronts in semiconductor superlattices*, Physical Review E **64** (2001), 036204-1–036204-9.

[5] A. Carpio, L.L. Bonilla, *Depinning transitions in discrete reaction-diffusion equations*, SIAM J. Appl. Math. **63** (2003), 1056–1082.

[6] A. Carpio, L.L. Bonilla, A. Luzón, *Effects of disorder on the wave front depinning transition in spatially discrete systems*, Physical Review E **65** (2002), 035207(R)-1–035207(R)-4.

[7] L.L. Bonilla, H.T. Grahn, *Nonlinear dynamics of semiconductor superlattices*, Reports on Progress in Physics **68** (2005), 577–683.

[8] J.I. Arana, L.L. Bonilla, H.T. Grahn, *Photo-excited semiconductor superlattices as constrained excitable media: Motion of dipole domains and current self-oscillations*, Physical Review B (2010), 035322-1–035322-8. LANL preprint cond-mat/arXiv:0912.4897.

Multi-scale approach for resonance effects in metamaterials.

Guy Bouchitté

Introduction

It is now commonly admitted that obstacles made of metallic or dielectric inclusions placed periodically in a suitable way can behave like homogeneous materials with negative refractive index (or other rather unexpected exotic properties). The aim of the talk is to present several 3D situations where such behaviors can be recovered rigorously by using multi-scale methods:

- High conductivity fibers with very small filling ratio (negative effective permittivity [1, 2, 3, 4, 5])

- High contrast dielectric inclusions (artificial magnetism and negative permittivity [6, 7, 8, 9, 10, 11])

- Pendry metallic split ring structures (see [12, 13, 14])

In all these cases, the key point relies on a spectral problem in the periodic cell which accounts internal resonances and allows to describe small scale oscillations of the electromanetic field. Due to the extreme values of the permittivity in the inclusions, these micro-resonances are compartible with a possibly large incident wavelength. The macroscopic behavior of the photonic crystal is then identified by using classical homogenization techniques.

In this report we will only present the case of a scattering body made of high conductivity metallic fibers and we will explain how negative effective permittivity tensors can be reached by choosing suitably the disposition, the size and the conductivity of the fibers.

Construction of the structure (metamaterial)

The metamaterial will exhibit two different microscopic scales. Its construction is realized in two steps.

Step 1. Recently in [3] a new homogenization theory was proposed for a bounded obstacle made of periodically disposed parallel high conducting metallic fibers of finite length and very thin section. Although the resulting constitutive law is non local, a cut-off frequency effect could be evidenced when fibers become infinitely long (see [2]).

Let us start by considering such a finite $3D$ scatter filled with periodically disposed $\mathbf{e_3}$-parallels metallic rods with very small radius a and high conductivity σ. The radius a is assumed to be infinitesimal with respect to the period d so that the filling ratio θ vanishes in the limit process. more precisely

Assumptions. In this model we assume that:

i) $d^2 \ln a \to \gamma^{-1}$ where the constant γ represents the average capacity of the rods per unit of volume.

ii) $\sigma\,\theta \to \kappa$ where $\theta = \pi \frac{a^2}{d^2}$ and κ represents the conductivity averaged over the scatter (since $\theta \to 0$, we have $\sigma \to +\infty$).

Under these scaling assumptions, it has been shown in [3] that the scatter illuminated by a mono chromatic incident wave (wave number k_0) has asymptotically a non-local behavior governed by the following system of equations:

$$(1) \qquad \begin{cases} \operatorname{curl} E = i\omega\,\mu_0\,H & \text{on } \mathbb{R}^3 \\ \operatorname{curl} H = -i\omega\,\varepsilon(E + i\,J\,e_3) & \text{on } \mathbb{R}^3 \\ \frac{\partial^2 J}{\partial x_3^2} + (k_0^2 + \frac{2i\pi\gamma}{\kappa})\ J \ = \ 2i\pi\gamma\ E_3 & \text{on } \Omega \\ \frac{\partial J}{\partial x_3} = 0 & \text{on } \omega_L^{\pm} \end{cases}$$

where $\Omega := \mathcal{D} \times [-L/2, L/2]$ and $\omega_L^{\pm} = \mathcal{D} \times \{\pm L/2\}$, and J represents the bulk average of the vertical displacement current induced in the fibers.

Step 2. Now we design a second device by repeating periodically photonic components of small size and of the same kind as the one constructed in Step 1. More precisely the periodic obstacle Σ_η is given by

$$(2) \qquad \Sigma_\eta \ = \ \Omega \cap \left(\bigcup_{i \in \mathbb{Z}^3} \eta(i + \Sigma) \right),$$

where $\Sigma = D \times (-h/2, h/2)$ is a cylinder strictly contained in the unit cell Y. Here D is a connected subdomain of $(-1/2, 1/2)^2$ and $h < 1$ denotes the height. The upper and lower basis of Σ are denoted $D^{\pm}$. Their rescaled periodic counterparts are called $D_\eta^{\mp}$. Applying directly the previous limit model on each component of Σ_η on which we plug the system (1), we are led to a global diffraction problem described by a triple (E_η, H_η, J_η) such that:

$$(3) \qquad \begin{cases} \operatorname{curl} E_\eta = i\omega\mu_0 H_\eta & \text{on } \mathbb{R}^3 \\ \operatorname{curl} H_\eta = -i\omega\varepsilon_0(E + i\,\mathbf{1}_{\Sigma_\eta}\,J_\eta\,\mathbf{e_3}) & \text{on } \mathbb{R}^3 \\ \frac{\partial^2 J_\eta}{\partial x_3^2} + \left(k_0^2 + \frac{2i\pi\gamma}{\kappa}\right)\ J_\eta = 2i\pi\gamma\,E_\eta \cdot \mathbf{e_3} & \text{on } \Sigma_\eta \\ \dfrac{\partial J_\eta}{\partial x_3} = 0 & \text{on } D_\eta^{\pm} \\ + \text{ radiations conditions at infinity} \end{cases}$$

where $\mathbf{1}_{\Sigma_\eta}$ denotes the function equal to 1 on Σ_η and zero otherwise.

In the perspective of obtaining a new effective law in the limit as $\eta \to 0$, our aim is to identify two-scale limits (E_0, H_0, J_0) of (E_η, H_η, J_η). The macroscopic electric and magnetic fields will be identified in the limit $\eta \to 0$ as

$$(4) \qquad E(x) = \int_Y E_0(x, y)\,dy\ , \quad H(x) = \int_Y H_0(x, y)\,dy\ .$$

Multiscale Analysis

By classics arguments of two-scale convergence, one checks that system (3) leads to the following cell problem for $(E_0(x,\cdot), H_0(x,\cdot), J_0(x,\cdot)$:

$$(5)\qquad \begin{cases} \operatorname{curl}_y E_0 \;=\; \operatorname{curl}_y H_0 = 0, \quad \operatorname{div}_y H_0 = 0\ , \\ \operatorname{div}_y(E_0 + \mathbf{1}_\Sigma J_0) = 0\ ,\ J_0 = J_0(y_1,y_2) \\ J_0 = \frac{2i\pi\gamma}{k_0^2+\frac{2i\pi\gamma}{\kappa}}\,\frac{1}{h}\int_{-h/2}^{h/2} E_0(y_1,y_2,y_3)\cdot \mathbf{e_3}\ dy_3 \end{cases}$$

By the two first equations of (5), $H_0(x,\cdot)$ is constant and we can write $E_0(x,\cdot)$ in term of a suitable periodic scalar potential $\Phi(x,\cdot)$:

$$H_0(x,y) = H(x) \quad , \quad E_0(x,y) = E(x) + \nabla_y \Phi(x,y)\ .$$

By the two last equations of (5), Φ satisfies

$$(6)\qquad \Delta_y \Phi = i\ J_0\,(\delta_{D^+} - \delta_{D^-})\ , \quad J_0 = \frac{2i\pi\gamma}{k_0^2+\frac{2i\pi\gamma}{\kappa}}\,(E_3 + [\Phi]_h)$$

where
$[\Phi]_h(\cdot,y_1,y_2) := \dfrac{1}{h}\Big(\Phi(\cdot,y_1,y_2,\dfrac{h}{2}) - \Phi(\cdot,y_1,y_2,-\dfrac{h}{2})\Big)$

Micro-resonator problem

We introduce the operator $B_h : w \in L^2(D) \mapsto [\varphi]_h(y_1,y_2)$ where φ is the unique Y-periodic solution of $-\Delta\varphi \;=\; w\,(\delta_{D^+} - \delta_{D^-})$. It is a linear positive compact selfadjoint operator and by (6), we see that $j_0(x,\cdot)$ satisfies the spectral equation:

$$(7)\qquad B_h(J_0) - \left(\frac{k_0^2}{2\pi\gamma} + \frac{i}{\kappa}\right) J_0 \;=\; -i\,E_3(x)\ .$$

Let $\nu_0^2 > \nu_1^2 \geq \nu_2^2 \cdots \geq \nu_n^2$ be the (real positive) eigenvalues of B_h ($\nu_n^2 \to 0$ as $n \to \infty$) and let $\{\varphi_n \;:\; n \in \mathbb{N}\}$ an associated orthonormal basis of $L^2(D)$. Then the solution of (7) is given by

$$(8)\qquad J_0(x,y_1,y_2) \;=\; i\,E_3(x)\,\chi(\omega,y_1,y_2)$$

with $\chi(\omega,y_1,y_2) := \sum_n c_n\varphi_n\ , \quad c_n = \frac{\int_D \varphi_n}{\frac{k_0^2}{2\pi\gamma}-\nu_n^2+\frac{i}{\kappa}}$

Effective permittivity

Exploiting (8)(9), the limit of the term $J_\eta\,\mathbf{1}_{\Sigma_\eta}$ in the second equation of (3) can be identified as the average $\int_\Sigma J_0(x,y_1,y_2)\,dy_1dy_2 \;=\; i\,h\,\Lambda(\kappa,\gamma,\omega)\,E_3(x)$, where

$$(9)\qquad \Lambda(\kappa,\gamma,\omega) \;:=\; \int_D \chi(\omega,y_1,y_2)\,dy \;=\; \sum_n \frac{(\int_D \varphi_n)^2}{\frac{k_0^2}{2\pi\gamma}-\nu_n^2+\frac{i}{\kappa}}$$

Thus the limit system reads

$$\begin{cases} \operatorname{curl} E = i\omega\mu_0\,H \\ \operatorname{curl} H = -i\omega\varepsilon_0\varepsilon^{eff}\,E \end{cases}$$

with ε^{eff} is the diagonal tensor given by

$$\varepsilon_{11}^{eff} = \varepsilon_{22}^{eff} = 1 \quad , \quad \varepsilon_{33}^{eff} = 1 - h\,\Lambda(\kappa, \gamma, \omega) \tag{10}$$

Thus we are led to a local effective law described by a permittivity tensor that we can explicit as a function of the frequency. By (9) the eigenvalues of this tensor have real part changing of sign and possibly very large within some range of frequencies. We refer to [5] for futher details and for a complete demonstration of the convergence result.

Notice that we may also generalize the previous construction by mixing three families of metallic fibers composants each of them being disposed alternatively in the three directions of axis. That way we will reach all effective tensors of the kind

$$\varepsilon^{\text{eff}} = \begin{pmatrix} 1 - h_1\,\Lambda_1(\omega) & 0 & 0 \\ 0 & 1 - h_2\,\Lambda_2(\omega) & 0 \\ 0 & 0 & 1 - h_3\,\Lambda_3(\omega) \end{pmatrix} ,$$

where the parameters h_i and fonctions $\Lambda_i(\omega)$ are computed according to the particular geometry and electromagnetic properties of each family of inclusions.

Conclusions

By considering a complex structure consisting of periodically disposed (period η) sytems of small arrays (size $d \ll \eta$) of parallel disconnected fibers of length $l \ll \eta$, we can construct a metamaterial showing micro-resonances effects for large wavelength incident field ($\lambda \gg \eta$). Such a metamaterial is characterized by a local effective permittivity tensor with possibly real negative eigenvalues (band gaps of frequencies). By tuning the geometrical parameters of the micro-fibers (filling ratio, conductivity, orientation of the fibers), we can reach (at least theoretically) a wide range of metamaterials including any one characterized by an *arbitrary real symmetric permittivity tensor*.

References

[1] J.B. Pendry, A.J. Holden, W.J. Stewart, and I. Youngs, *Extremely low frequency plasmons in metallic mesostructures*, Phys. Rev. Lett., **76** (1996), pp. 4773–4776.

[2] G. Bouchitté, and D. Felbacq, *Homogenization of a set of parallel fibers, Waves in Random Media*, Vol. **7**, (1997), 1–12.

[3] G. Bouchitté, and D. Felbacq, *Homogenization of a wire photonic crystal: the case of small volume fraction*, SIAM J. Appl. Math. **66**, 2061 (2006)

[4] G. Bouchitté, D. Felbacq, and F. Zolla, , *Bloch vector dependence of the plasma frequency in metallicphotonic crystals*, Phys. Rev. E **74**, 056612 (2006)

[5] G. Bouchitté, and C. Bourel, *submitted*

[6] S. O'Brien, and J.B. Pendry, *Photonic band-gaps effects and magnetic activity in dielectric composites*, J. Phys.: Condens. Matter **14** (2002) 4035-4044.

[7] G. Bouchitté, and D. Felbacq, *Left handed media and homogenization of photonic crystals*,' Optics letters, **30** (2005), 10.

[8] D. Felbacq, and G. Bouchitté, *Homogenization of wire mesh photonic crystals embdedded in a medium with a negative permeability*, Phys. Rev. Lett. **94**, 183902 (2005)

[9] G. Bouchitté, and D. Felbacq, *Homogenization near resonances and artificial magnetism from dielectrics*, C. R. Math. Acad. Sci. Paris **339** (2004), 377–382.

[10] G. Bouchitté, and D. Felbacq, *Negative refraction in periodic and random photonic crystals*, New J. Phys. 7 159 10.1088/ (2005)
[11] Bouchitté, G., Bourel C. and Felbacq,D, Homogenization of the 3D Maxwell system near resonances and artificial magnetism. CRAS Volume 347, Issues 9-10, May 2009, Pages 571-576
[12] S. O'Brien and J.B. Pendry, *Magnetic activity at infrared frequencies in structured metallic photonic crystals*. J. Phys. Condens. Mat., **14**: 6383-6394, 2002.
[13] R.V. Kohn and S. Shipman, *Magnetism and homogenization of microresonators*. Siam Multiscale Model. Simul. **7** (2008), no. 1, 62-92.
[14] G. Bouchitté, and B. Schweizer, *Homogenization of Maxwell equations with split rings*, to appear in Multiscale Model. Simul.

Rearrangement and Convection

Yann Brenier

A crude model of convection. Let us introduce the following discrete scheme as a crude model of convection: we consider a vertical column of fluids with N equally spaced grid points $a_1 < a_2 < ... < a_N$. At each discrete time $t = hn$, $n = 0, 1, 2, ...$, the temperature at elevation a_i is denoted by y_i^n. A heat source is located at each elevation a_i and denoted by $G(a_i)$ where G is a given smooth function. Then, the evolution of the temperature is made of two steps:
i) a predictor step which takes into account the heat source:
$\tilde{y}_i^{n+1} = y_i^n + h\, G(a_i)$,
ii) a corrector step which rearranges the temperature field in increasing order so that the cold fluid instantaneously goes to the bottom and the hot fluid goes to the top:
$y_{n+1} = R[\tilde{y}_{n+1}]$,
where R denotes the rearrangement operator (i.e. sorting in increasing order).

Convergence analysis. The numerical scheme has a unique continuous limit $y(t, a)$ which can be shown to be the solution of the subdifferential equation:

$$G(a) \in \partial_t y + \partial \Psi[y] \tag{1}$$

where $\Psi[y] = 0$ if $y = y(t, a)$ is non decreasing as a function of a
and $\Psi[y] = +\infty$ otherwise. This equation is well-posed in the space L^2. The pseudo-inverse $u(t, y)$ defined by $u(t, y(t, a)) = a$ can also be shown to be a Kruzhkov entropy solution to the scalar conservation law

$$\partial_t u + \partial_y(g(u)) = 0, \tag{2}$$

with flux $g(a) = \int_0^a G(b)db$.

Multidimensional rearrangements with convex potential. There is a multidimensional generalization of the concept of rearrangement in increasing order which is closely related to optimal transport theory: given a smooth bounded domain $D \subset R^d$, any $z \in L^2(D, R^d)$ has a unique rearrangement $R[z] \in L^2(D, R^d)$ for which there is a convex lsc p such that $\nabla p(x) = R[z]$ almost everywhere in D. (cf. [1], see also [4].) Thanks to this multidimensional rearrangement result, it is straightforward to get a generalization of the model in higher dimension, where it is understood that:
-$y(t, x) \in R^d$ (generalized temperature) is now a vector field valued in R^d,
-the source term $G = G(x)$ is also valued in R^d and has bounded derivatives.
For this multidimensional extension of the model, we can show the global existence of a generalized solution $y(t, x) \in R^d$ with a convex potential, valued in $C^0([0, +\infty[, L^2(D, R^d))$, in the sense:

$$\frac{d}{dt}\int_D f(y(t,x))dx = \int_D (\nabla f)(y(t,x)) \cdot G(x)dx \tag{3}$$

for all smooth function f such that $|f(x)| \leq 1 + |x|^2$. Notice that the formulation (3) is "self-consistent", thanks to the rearrangement theorem. Indeed, the knowledge of $f \to \int_D f(y(t, x))dx$ for all suitable f is sufficient to recover $y(t, x)$ entirely, as a map with convex potential. However, uniqueness issues are essentially unsolved except in the case $d = 1$ and $G(a) = -a$, where, in different ways, maximal monotone operator theory can be used.

Derivation from the Navier-Stokes equations with Boussinesq approximation. Finally, our multidimensional model can be seen as the singular limit of the convection model

$$\epsilon(\partial_t + v \cdot \nabla - \Delta)v + \nabla p = f \ , \quad (\partial_t + v \cdot \nabla)f = G \ , \ \nabla \cdot v = 0,$$

as ϵ goes to zero, where the unknowns $f = f(t, x) \in R^d$, $v = v(t, x) \in R^d$, $p = p(t, x) \in R$ depend on t and $x \in R^d$ and $G = G(x) \in R^d$ is given. The limit system, that we call Hydrostatic Boussinesq (HB) model,

$$\nabla p = f \ , \quad (\partial_t + v \cdot \nabla)f = g \ , \ \nabla \cdot v = 0,$$

is locally well posed under the requirement that $p = p(t, x)$ is a uniformly strictly convex smooth function in x. In this local regime, the convergence can be proven thanks to a suitable 'relative entropy' argument

For more details, we refer to the recent papers [2] and [3], and the references included in these papers, in particular by Gregoire Loeper on the semigeostrophic equations.

References

[1] Y. Brenier, *Polar factorization and monotone rearrangement of vector-valued functions.*, Comm. Pure Appl. Math. **44** (1991), 375–417.
[2] Y. Brenier, *Optimal transport, convection, magnetic relaxation and generalized Boussinesq equations*, J. Nonlinear Sci. **19** (2009), 547–570.

[3] Y. Brenier, and M. Cullen, *Rigorous derivation of the X-Z semigeostrophic equations*, Commun. Math. Sci. **7** (2009), 779–784.
[4] C. Villani, *Topics in optimal transportation*, Graduate Studies in Mathematics **58**, American Mathematical Society, Providence, (2003).

Mathematical crystallography of the structural transitions of viruses

Paolo Cermelli

(joint work with Giuliana Indelicato, Simone Racca, Reidun Twarock, Giovanni Zanzotto)

Structural capsid transitions are important for virus function, as in maturation or infection processes, and have been the object of recent analyses from both the experimental and theoretical viewpoints [14], [15], [16], [6], [7], [8]. In this work we explore how crystallographic notions which are useful in the kinematics of reconstructive structural phase transformations in crystalline solids [5], [17], [13], [3], [10], can be adapted for the investigation of viral transitions.

We start from the fact that capsid configurations can be well approximated by suitable double-shell point configurations in 3D with icosahedral symmetry [8]. By adapting classical notions in the theory of quasicrystals [11], [9], we first show how such structures can be obtained as projections to 3D space of suitable subsets of the icosahedral (i.e. the simple-, body-centered-, and face-centered-cubic) Bravais lattices in 6D. The transitions between two configurations of a virus can then be studied in terms of transitions between two 6D lattices. For this purpose we consider the 6D analogs of the 'Bain-like' deformations, which constitute an important class of transition paths involving minimal intermediate symmetry reduction and minimal strain, and related concepts [2], [13], [4], [12], [1].

As a specific example illustrating our approach, we consider the Cowpea Chlorotic Mottle virus (CCMV), whose capsid structures have been investigated in some detail [6], [8]. The experimental observations on the CCMV capsid are compatible with: (a) a set of two pre-transition configurations; and (b) a set of ten post-transition configurations. Each such set of double-shell icosahedral structures gives respectively the possible initial and final configurations in the transition path, which is at present unknown, and here we perform a systematic analysis of all the possible 6D Bain-like paths between the given start and end configurations. We do so by calculating suitable finite subsets of the integral normalizers of the maximal subgroups of the integral representations of the icosahedral group in 6D (cf. [18]), and by suitably measuring the strain such deformations induce on the 3D shell structures.

The results we obtain from this analysis give a ranking of likely transition mechanisms for the CCMV virus confugurations, based on the requirements of minimal symmetry loss at intermediate configurations and minimal overall strain.

The approach we propose suggests a general method for the investigation and prediction of possible capsid distortion paths, which may give guidelines for future experimental or numerical work on viral transitions.

References

[1] P. Alippi, P. M. Marcus, M. Scheffler, *Strained Tetragonal States and Bain Paths in Metals*, Phys. Rev. Lett., **78**/20, (1997).

[2] E. C. Bain, *The Nature of Martensite*, Trans. AIME **70**, (1924).

[3] K. Bhattacharya, S. Conti, G. Zanzotto, J. Zimmer, *Crystal symmetry and the reversibility of martensitic transformations*, Nature **428** (2004).

[4] C. Capillas, J. M. Perez-Mato, M. I. Arroyo, *Maximal symmetry transition paths for reconstructive phase transitions*, J. Phys.: Condens. Matter **19** (2007).

[5] J.W. Christian, *The theory of transformations in metals and alloys*, Pergamon Press (2002).

[6] T. Keef, R. Twarock, *New insights into viral architecture via affine extended symmetry groups*, Computational and Mathematical Methods in Medicine **9**, (2008).

[7] T. Keef, R. Twarock, K.M. Elsawy, *Blueprints for viral capsids in the family of Papovaviridae*, J. Theor. Biol. **253**, (2008).

[8] T. Keef, R. Twarock, *Affine extensions of the icosahedral group with applications to the three-dimensional organisation of simple viruses*, J. Math. Biol. **59**, (2009).

[9] L. S. Levitov, J. Rhyner, *Crystallography of quasicrystals; application to icosahedral symmetry*, J. Physique **49**, (1988).

[10] M. Pitteri, G. Zanzotto, *Continuum Models for Phase Transitions and Twinning in Crystals*, CRC/Chapman and Hall, (2002).

[11] M. Senechal, *Quasicrystals and geometry*, Cambridge University Press, (1995).

[12] H. Sowa, E. Koch, *Group-theoretical and geometrical considerations of the phase transition between the high-temperature polymorphs of quartz and tridymite*, Acta Cryst. **A58** (2002).

[13] P. Toledano, V. Dmitriev, *Reconstructive Phase Transitions*, World Scientific Publishing Company (1996).

[14] R. Twarock, *A tiling approach to virus capsid assembly explaining a structural puzzle in virology*, J. Theor. Biol. **226**, (2004).

[15] R. Twarock, *The architecture of viral capsids based on tiling theory*, J. Theor. Medicine **6**, (2005).

[16] R. Twarock, *A Mathematical Physicist's Approach to the Structure and Assembly of Viruses*, Phil. Trans. Royal Soc. A **365**, (2006).

[17] C.M. Wayman. *Introduction to the crystallography of martensite transformations*, Macmillan, (1964).

[18] F. Wijnands, *An algorithm to find generators for the normalizer of an n-dimensional crystalographic point group in* $GL(n, \mathbb{Z})$, J. Phys. A: Math. Gen. **24**, (1991).

Crack kinking in planar elasticity

Antonin Chambolle

(joint work with Gilles Francfort, Jean-Jacques Marigo)

We consider a planar linear-elastic brittle material. In the classical theory proposed by Griffith [6], a fracture increases in order to release an amount of energy which is dissipated into the system. Then, one assumes that the dissipation for creating a crack of a certain length is proportional to this length, with a factor G_c known as the "toughness" of the material. If one neglects all other possible ways of dissipating energy (e.g., thermal dissipation), one arrives to the following model.

- The setting is a (smooth) reference configuration $\Omega \Subset \mathbb{R}^2$ and an increasing boundary condition $u^0(t)$ on $\partial\Omega$ ("hard device"— could also be on some part, or also be a force "soft device"). Ex: $u^0(t) = tU^0$, $U^0 \in H^{1/2}(\partial\Omega)$.
- The crack path $\gamma(\ell)$, $\ell = \text{length}(\gamma(\ell)) \geq 0$, is supposed to be known and the fracture grows continuously along γ.
- The elastic energy associated to a boundary displacement $u^0(t)$ and a crack of length ℓ is

$$W(t,\ell) \;=\; \min_{\substack{u=u^0(t)\\ \text{on } \partial\Omega}} \frac{1}{2}\int_{\Omega\setminus\gamma(\ell)} Ae(u) : e(u)\,dx$$

  where $u \in H^1_{\text{loc}}(\Omega \setminus \gamma(\ell))$ and A is the Hooke's law, given (in isotropic elasticity) by $\sigma = Ae(u) = 2\mu e(u) + \lambda \text{Tr} e(u)\, I$.
- The *energy release rate* is

$$G(t,\ell) \;=\; -\frac{\partial W(t,\ell)}{\partial \ell} \;\geq\; 0$$

- The evolution must obey the axioms:
  (1) *(Irreversibility)* $t \mapsto \ell(t)$ is nondecreasing,
  (2) *(Stability)* $G(t,\ell(t)) \leq G_c$,
  (3) *(Energy-dissipation balance)* $(G(t,\ell(t)) - G_c)\dot{\ell}(t) = 0$

This model suffers a few drawbacks. In particular, it is unable to predict the crack initiation, nor its trajectory. The issue of crack initiation has been analysed in [4]. Let us comment on the issue of predicting the trajectory. We consider more particularly the problem of "crack kinking". The situation is as follows: an initial crack γ^i is ending at $0 \in \Omega$ by a straight segment. Then, it is known since Grisvard [7] that at the tip, the displacement u has the form

$$u \;=\; K_1\Phi_1 \;+\; K_2\Phi_2 \;+\; v$$

where $v \in H^2(\Omega \setminus \gamma^i)$ while Φ_i are 1/2-homogeneous and correspond to the "mode 1"-opening (which is symmetric) and "mode 2"-opening (a pure shear). The coefficients K_i, called "stress intensity factors" (SIF), are related to the energy release rate as follows: $G \sim K_1^2 + K_2^2$ if the fracture grows in its direction.

If the crack is loaded in a symmetric way, $K_2 = 0$ and it is supposed to grow smoothly. If not, one has $K_2 \neq 0$ and one expects it to "kink", that is, to change brutally its direction. Two competing criteria are classically used to determine the angle θ that the new crack will make with the initial crack:

- "$G_{\max}$": the idea is to compute, for infinitesimal straight add-cracks at the tip 0, the release rate $G(\theta) = -\lim_{\varepsilon\to 0}(W(\varepsilon,\theta) - W(0))/\varepsilon$,

$$W(\varepsilon,\theta) \;=\; \min_{\substack{u=u^0(t)\\ \text{on } \partial\Omega}} \frac{1}{2}\int_{\Omega\setminus(\gamma^i\cup\varepsilon[0,X_\theta])} Ae(u) : e(u)\,dx,$$

  where $X_\theta = (\cos\theta, \sin\theta)$. It depends on the angle θ between the add-crack and the initial crack γ^i. One then looks for the angle θ which maximizes

this release rate and if it is equal to G_c the fracture starts growing in that direction.

- "PLS" (Principle of local symmetry): the idea is that after the kinking the fracture should be stable and in particular not "kink" again: hence on looks for an angle θ such that $K_2^*(\theta) = 0$ where $K_i^*(\theta)$ are the SIFs at the tip of the infinitesimal add-crack $\varepsilon[0, X_\theta]$. One then uses the corresponding release rate $G_{\rm PLS}$.

The issue is that it is widely accepted that these criteria are incompatible (although this is only a conjecture, which supported by an asymptotic development at zero, and a numerical estimation of $(K_1^*(\theta), K_2^*(\theta))$ as a (linear) function of (K_1, K_2), see [5, 1, 8]). In any case, it is proved that they can be compatible only for a finite number of angles.

Doing a suitable blow-up analysis at 0, we define in [3] a "generalized energy-release rate" at the tip, which depends on an arbitrary (connected) add-crack pattern Σ. It means that we consider the crack $\gamma^i \cup \varepsilon\Sigma$ for $\varepsilon > 0$ small, and compute the normalized release of energy as $\varepsilon \to 0$.

Then, we say that a crack is unstable as soon as for all $\varepsilon > 0$ small enough, it is possible to find a small add-crack which lowers the global energy+dissipation. In this case, we can show that a crack loaded in a nonsymmetric way ($K_2 \neq 0$) is unstable "before" what both "PLS" and "$G_{\max}$" criteria predict. The conclusion is that it should not grow according to classical Griffith's laws (and most probably, not in a continuous way). Even if there is a doubt that physical systems which perfectly obey these laws exist, this analysis applies to the evolutions described in [2], restricted to the planar case.

References

[1] M. Amestoy and J.-B. Leblond, *Crack paths in plane situations. II. Detailed form of the expansion of the stress intensity factors*, Internat. J. Solids Structures, **29**(4) (1992) 465–501.

[2] B. Bourdin, G. A. Francfort, and J.-J. Marigo, *The variational approach to fracture*, Springer, 2008.

[3] A. Chambolle, G. Francfort, and J.-J. Marigo, *Revisiting energy release rates in brittle fracture*, to appear in JNLS (2010).

[4] A. Chambolle, A. Giacomini, and M. Ponsiglione, *Crack initiation in brittle materials*, Arch. Ration. Mech. Anal., **188**(2) (2008) 309–349.

[5] B. Cotterell and J. R. Rice, *Slightly curved or kinked cracks*, International Journal of Fracture, **16**(2) (1980) 155–169.

[6] A. A. Griffith, *The phenomena of rupture and flow in solids*, Phil. Trans. Roy. Soc. London, CCXXI-A (1920) 163–198.

[7] P. Grisvard, *Singularités en elasticité*, Arch. Rational Mech. Anal., **107**(2) (1989) 157–180.

[8] J.-B. Leblond, *Crack paths in plane situation – I, General form of the expansion of the stress intensity factors*, Int. J. Solids Struct., **25** (1989) 1311–1325.

A reappraisal of the Andersen-Parrinello-Rahman method from a continuum mechanics point of view

Antonio DiCarlo
(joint work with Matteo Paoluzzi, Paolo Podio-Guidugli, Marco Ribezzi-Crivellari)

Continuum Physics and Molecular Dynamics. Multiscale approaches are key to understanding phenomena in fields as different as biology, materials science, fluid mechanics, and chemistry. Finding accurate and efficient methods for bridging the gap between the atomistic time and space scales accessible by computer simulation, the mesoscopic scale addressed by coarse-grained models, and the macroscopic domains described by continuum mechanics is key for modelling and computing multiscale properties. The arena where molecular dynamics (MD)—and, more generally, atomistic models—meet with concepts and techniques from continuum physics is nowadays one of the most exciting and promising areas for innovative mathematical modelling. The interplay between atomistic and continuum physics is vital, and it should work both ways: while fine theories would hopefully produce coarser theories with sound constitutive information, coarse theories provide a well-structured target to fine ones. This greatly helps in culling the effective behaviour of interest out of the bewildering mass of unstructured microscopic information.

In a way, the attitude we advocate is a return to the origins of continuum physics. Strange as it may appear to us, many of its founding fathers strongly believed in the necessity of an underlying *discrete* structure of matter—while having in mind a very naïve molecular picture of it. In the closing Section 134 of his treatise on three-dimensional elasticity [1] Lamé identified that theory as *molecular physics*:

> Nous terminons cette Leçon, et le Cours que nous avons entrepris, par quelques réflexions sur la constitution intérieure des corps solides. [. . . T]outes les questions relatives à la Physique moléculaire ont été rétardées, plutôt qu'avancées, par l'extension, au moins prématurée sinon fausse, des principes et des lois de la Mécanique céleste.

The APR Method for Molecular Dynamics. In classical MD the equations of motions for a finite set of Newtonian interacting particles are integrated numerically, and properties of the system are obtained from the generated phase-space trajectories. For practical reasons, the number of particles in the computational cell is nowadays restricted to several millions. Thirty years ago, when Andersen wrote his seminal paper [2], the practicable number was just one thousand. This more than thousandfold increase, however prodigious, is trifling when compared with the extra factor needed to bridge the abyss separating 10^6 from an Avogadro number ($\sim 6{\cdot}10^{23}$) of particles: from a macroscopic point of view, an attomole (10^{-18} mol) is negligibly larger than a zeptomole (10^{-21} mol). If such minuscule aggregates

were simulated in isolation, their bulk properties would be polluted—if not altogether obliterated—by overwhelming surface effects. Hence, the common practice used to compute bulk properties is to (imagine to) fill asymptotically the entire space (assumedly Euclidean) by periodically repeating a unit parallelepipedal cell of finite size containing a finite—and relatively small—number of particles. This makes the boundary recede to infinity and obliterates any surface effects.

However, if the size and shape of the computational cell are fixed once for all and the number of particles per cell is kept constant (as implied by periodicity), many situations of obvious interest turn out to be inaccessible to direct simulation and some materials phenomena of major interest—such as phase changes—are simply inhibited. It is desirable, for instance, to be able to perform simulations at constant temperature and/or pressure, as Andersen pointed out in [2]. But this is not feasible with the above described technique, since it keeps constant the number of particles, the volume of the cell they invade and their total energy, thus producing (approximate) averages over a microcanonical ensemble. As further observed by Parrinello and Rahman in [4], changes in the shape of the periodic cell play an essential role in crystal structure transformations. For example, in a plane four points at the vertices of a square cell together with one at the centre generate a square lattice, which can become a lattice of equilateral triangles only if the square cell is allowed to transform into a rectangular cell having aspect ratio $1:\sqrt{3}$.

To remove this impediment, in 1979 H.C. Andersen devised a way to allow the cell volume to evolve under a time-dependent dilation [2]. M. Parrinello and A. Rahman immediately extended Andersen's idea to general linear transformations, allowing also the cell shape to fluctuate and evolve in time [3, 4]. In the Andersen-Parrinello-Rahman (APR) method, the prototype cell is allowed to deform in a very orderly way, being assumed to stay parallelepipedal. Therefore, its evolution may be parameterized by n vector-valued maps $\tau \mapsto (\mathbf{a}_1(\tau), \ldots, \mathbf{a}_n(\tau))$ that yield cell edges as a function of time or, equivalently, by the single tensor-valued map $\tau \mapsto \mathbf{F}(\tau)$ such that $\mathbf{a}_\ell(\tau) = \mathbf{F}(\tau)\,\mathbf{e}_\ell \;\; (1 \le \ell \le n)$, $(\mathbf{e}_1, \ldots, \mathbf{e}_n)$ being a given vector basis. The instantaneous *cell deformation tensor* $\mathbf{F}(\tau)$ is assumed to be invertible at all time τ, so that the cell never degenerates. The instantaneous radius vector $\mathbf{r}_i(\tau)$ of the i-th particle is then given as

$$\mathbf{r}_i(\tau) = \mathbf{F}(\tau)\,\mathbf{s}_i(\tau) \quad (1 \le i \le N)\,,$$

where $\mathbf{s}_i(\tau)$ is the i-th instantaneous *scaled radius vector* and N is the number of particles in the cell. The original proposal by Andersen is tantamount to the hypothesis that $\mathbf{F}$ takes only spherical values: $\mathbf{F}(\tau) = \lambda(\tau)\,\mathbf{I}$, where the scalar $\lambda(\tau) > 0$ is the instantaneous *cell dilation* and $\mathbf{I}$ the identity tensor.

Beyond the APR Lagrangian. Both $\mathbf{s}_i$ $(i = 1, \ldots, N)$ and $\mathbf{F}$ are now regarded as independent variables, whose evolution is governed by an extended Lagrangian, subtly introduced by Andersen and generalised by Parrinello and Rahman. The APR Lagrangian stems from a shrewd, but unwarranted hypothesis: the *kinetic*

decoupling of the cell DOFs from the particle DOFs. To quote Parrinello and Rahman themselves [4]:

> Whether such a Lagrangian is derivable from first principles is a question for further study.

After nearly thirty years, this foundational study was still to be done, since MD practitioners always considered the APR Lagrangian just as an expedient trick for generating the desired particle statistics—but see the very recent contribution from P. Podio-Guidugli [5].

On the contrary, we are now interested in the dynamics of the deforming computational cell per se, wishing to identify it with the body element of a Cauchy continuum. Seen from this perspective, APR-like Lagrangians embody the coupling between atomistic and continuum DOFs. Through extensive MD simulations using the standard "simplified" APR Lagrangian and some "corrected" versions of it, we plan to inquire how neglected kinetic couplings affect the fluctuations of the cell. Ultimately, we aim to construct atomistically informed approximations to a continuum by means of an array of interacting APR-like cells, simulated in parallel.

References

[1] G. Lamé, *Leçons sur la Théorie Mathématique de l'Elasticité des Corps Solides* (deuxième édition), Gauthier-Villars, Paris (1866).

[2] H.C. Andersen, *Molecular dynamics simulations at constant pressure and/or temperature*, Journal of Chemical Physics, **72** (1980), 2384–2393.

[3] M. Parrinello and A. Rahman, *Crystal structure and pair potentials: A molecular-dynamics study*, Physical Review Letters, **45** (1980), 1196–1199.

[4] M. Parrinello and A. Rahman, *Polymorphic transitions in single crystals: A new molecular dynamics method*. Journal of Applied Physics, **52** (1981), 7182–7190.

[5] P. Podio-Guidugli, *On (Andersen-)Parrinello-Rahman molecular dynamics, the related metadynamics, and the use of the Cauchy-Born rule* (submitted).

Interface Evolution in a Random Obstacle Model

Nicolas Dirr

(joint work with J. Coville, S. Luckhaus, P. Dondl, M. Scheutzow)

We consider the following semi-linear PDE with random coefficients, the so-called *Random Obstacle Model:*

$$\partial_t u(x,t,\omega) = \Delta u(x,t,\omega) + f(x,u(x,t,\omega),\omega) + F \quad \text{on } \mathbb{R}^n \tag{1}$$

$$u(x,0) = 0 \tag{2}$$

This is supposed to capture some features of an interface moving through a field of random obstacle: The graph of the function $u : \mathbb{R}^n \times \mathbb{R}^+ \to \mathbb{R}$, i.e. the set $\Sigma(t) := \{(x, u(t,x))\}$ is the interface. The surface tension, captured by the Laplacian in the equation, tries to keep the graph "flat." F is a constant driving force, driving the interface though the obstacles.

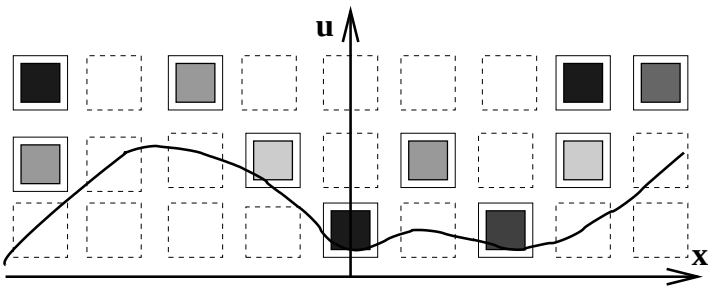

FIGURE 1. The random nonlinearity $f(x, u, \omega)$ describes the effect of obstacles with random strength. The strength of the random obstacles is indicated by the grey level, darker obstacles are stronger. f is negative on the obstacles and zero else.

The random nonlinearity $f(x, u, \omega) : \mathbb{R}^n \times \mathbb{R} \times \Omega \to \mathbb{R}$ models the field of soft obstacles. Loosely speaking, f is negative on an obstacle with a strength which is random, vanishes away from the obstacles. (See figure 1). The obstacles do not change with time.

More precisely, the random nonlinearity is constructed in the follwing way: Let ϕ be the mollification of a cylindrical obstacle of height and radius $0 < \delta < 1/4$ centered at zero, i.e. Φ smooth and nonnegative,

$$1_{[-(3\delta)/4,(3\delta)/4]\times B_{(3\delta)/4}(0)}(x, u) \leq \Phi(x, u) \leq 1_{[-\delta,\delta]\times B_\delta(0)}(x, u).$$

Then

$$f(x, u, \omega) = \sum\nolimits_{(i,j)\in\mathbb{Z}^n\times(\mathbb{Z}+\frac{1}{2})} \left(\mathbb{E}(\ell_{ij}) - \ell_{i,j}(\omega)(\omega)\right) \phi(x - i, u - j).$$

Here the random obstacle strength $(\ell_{i,j}(\omega))_{(i,j)\in\mathbb{Z}^n\times(\mathbb{Z}+\frac{1}{2})}$ are a family of independent identically distributed exponential random variables. (i.e. there exists $\lambda_0 > 0$ such that $\mathbb{P}\{\ell(i, j)(\omega) > r\} = e^{-\lambda_0 r}$ for $r \geq 0$). In certain situations the assumption on exponential tails of the strength can be modified. In general, the precise effects of the tail of the obstacle strength distribution is a topic of ongoing research. Note that f is not symmetric in this model and does not have average zero.

In the physics literature, a parabolic semi-linear equation with random coefficients like (1) is sometimes called Quenched Edwards Wilkinson model.

It is motivated in the following way: A very basic model for an interface (phase boundary, dislocation line in its slip plane etc) moving through an array of random obstacles (e.g. impurities, other dislocation lines) in an over-damped limit (inertial effects are neglected) is the gradient flow of the area functional plus a random bulk term. If so-called inner variations are considered, the resulting evolution law is *forced mean curvature flow*, where the forcing is random. For forced mean curvature flow and applications, in particular in the case of periodic forcing, we refer to [4], [2], [7]. If the interface is a graph and the gradient is sufficiently small, the evolution by forced mean curvature flow for the graph can be approximated heuristically by a semi-linear parabolic PDE as (1).

Related problems have found considerable interest in the physics community, see e.g. [9, 1].

Pinning or no pinning? The forcing F pushes the interface up, while the obstacles (which are not uniformly bounded) try to keep the interface down. Which effect wins?

For *periodic* $f(x,u)$ this is completely understood (see [8]). Here we ask whether, depending on F, $\lim_{t\to\infty} u(x,t)$ is finite (pinning) or infinite (no pinning). (Note that there are by construction no obstacles on $\{u=0\}$ so it is easy to see that always $\partial_t u \geq 0$) By the comparison principle for (1), any global non-negative stationary solution acts as barrier for (1,2), so it it is sufficient to consider existence or non-existence of solutions for

$$\begin{cases} 0 &= \Delta u(x,\omega) + f(x,u(x,\omega),\omega) + F \quad \text{on } \mathbb{R}^n \\ u(x) &\geq 0 \end{cases} . \tag{3}$$

We have the following results:

Theorem 1 [N.D., J. Coville, S. Luckhaus, see [3]] Let the space dimension $n=1$ and let u solve (3) on $[-N,N]$ with $u(-N)=u(N)=0$. Then there exist $F_0>0$, C and K such that for $F>F_0$

$$\mathbb{P}\Big(u(x) \geq KN - K|x| \text{ for all } x\in[-N,N]\Big) \geq 1 - Ce^{-\frac{N}{C}} \tag{4}$$

The result extends directly to higher dimensions if the model is a *discrete* version of (1), extending the discretization procedure used in the one-dimensional proof is work in progress. It says that nonnegative stationary solutions of the Dirichlet problem grow like the domain size for F large, i.e. the random obstacles cannot keep the solution down.

Theorem 1 implies the desired non-existence of a nonnegative stationary solution as corollary, as, by the comparison principle for the parabolic equation (1), any global non-negative stationary solution has to remain above the solution of the Dirichlet problems considered in Theorem 1:

Corollary 1 [$n=1$] There is almost surely no global non-negative stationary solution of (3).

Moreover we have a complementary result for existence of stationary solutions, i.e. pinning of evolving interfaces.

Theorem 2 [N.D., P. Dondl, M. Scheutzow, see [5]] Let $n=1,2$. There ex. $0<F_1$ such that for $0<F<F_1$, (3) has almost surely a solution with $\mathbb{E}[u(x,\omega)] = c<\infty$ for all $x\in\mathbb{R}^n$.

The idea of the proof is to decompose $\mathbb{R}^n\times\mathbb{R}^+$ in large cubes and to call a cube *open* if it contains an obstacle with strength larger than an approriately chosen cut-off. We would like to construct a Lipschitz-path w with Lipschitz constant depending on h/L, which crosses only open cubes. Mapping the cubes to sites on the integer lattice, this corresponds to asking whether the percolating cluster of open sites contains a Lipschitz graph. This question is answered affirmatively by a recent result on Lipschitz percolation, see [6], provided the probability of a cube being open is sufficiently large.

From w we are able to construct a function $u \geq 0$ such that

$$0 \geq \Delta u(x,\omega) + f(x,u(x,\omega),\omega) + F \quad \text{on } \mathbb{R}^n.$$

References

[1] Serguei Brazovsii and Thomas Nattermann: Pinning and sliding of driven elastic systems: from domain walls to charge density waves. Advances in Physics, vol. 53, no.2, 177-252, 2004.

[2] B. Craciun and K. Bhattacharya,, *Effective motion of a curvature-sensitive interface through a heterogeneous medium*, Interfaces Free Bound., **6**, (2004), 151–173.

[3] J. Coville, N. Dirr and S. Luckhaus. Non-existence of positive stationary solutions for a class of semi-linear PDEs with random coefficients. Submitted

[4] P. Cardaliaguet, P.L. Lions and P. E. Souganidis, *A* discussion about the homogenization of moving interfaces, J. Math. Pures Appl. **91** (2009), 339–363.

[5] Nicolas Dirr, Patrick W. Dondl, Michael Scheutzow: Pinning of interfaces in random media arXiv:0911.4254v1

[6] N. Dirr, P. W. Dondl, G. R. Grimmett, A. E. Holroyd, M. Scheutzow Lipschitz percolation arXiv:0911.3384v2

[7] N. Dirr, G. Karali, G. and N. K. Yip, *Pulsating wave for mean curvature flow in inhomogeneous medium*, European Journal for Applied Mathematics **19**, (2008), 661–699.

[8] N. Dirr and N. K. Yip, *Pinning and de-pinning phenomena in front propagation in heterogeneous media*, Interfaces Free Bound., **8**, (2006), 79–109.

[9] W. Kleemann, *Dynamic phase transitions in ferroic systems with pinned domain wall.* In: Abstracts from the Workshop "Phasenübergänge" held June 20–26, 2004, Organized by H.W. Alt, S. Luckhaus, E. Presutti and E.K.H. Salje, Oberwolfach Reports **1** (2004), 1587–1656.

Rolling Matter (space-filling packings)

Hans Herrmann

Since Apollonius of Perga we know that it is possible to fill space with circles of very different sizes. The self-similarity of this construction generates a power-law size distribution defining a fractal dimension. We will see that it is possible to generate also space-filling packings of disks in such a way that they can all roll sliplessly on each other. This is achieved using conformal transformations. Discrete families of different topologies can be classified algebraically. Aided by computers it has been possible to discover also a three dimensional packing that fulfils this property. Only one topology is known up to now allowing however for an infinity of rolling modes. Applications of these packings are models for turbulence and for tectonic gouge in seismic gaps. One can also construct random variants, study the energy spectrum and observe anomalous diffusion of tracer particles.

Figure 1 shows a 2d Apollonian packing. With S.S. Manna we calculated its fractal dimension to be 1.3057 +/- 0.0001 as published in [14]. In 1989 I constructed a much larger family of such packings of different topology and fractal dimension that also could serve as space-filling bearings as explained in detail in [6]. In [5] we showed with Giorgio Mantica and Daniel Bessis that there exist only two discrete families of different solutions for packings having only loops of four

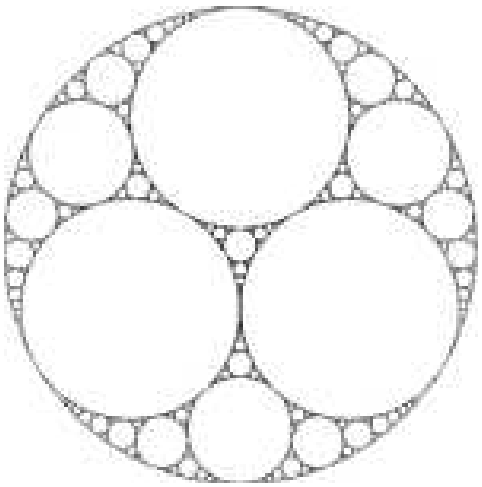

FIGURE 1

discs. The generalization to arbitrary even loop length was published with Gadi Oron in [16].

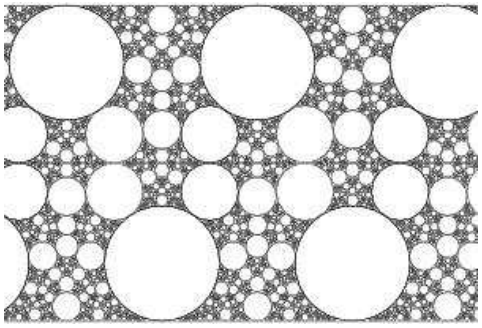

FIGURE 2

Figure 2 shows a configuration in the strip geometry (goes to infinity in horizontal direction) of the first family having loops of length 6 and the parameters n=m=0. It is obtained by a conformal map that consists iteratively of an inversion and a reflection. Only very specific radii for the original circles as well as for the inversion circles are allowed which gives the condition for the discrete families of possible solutions. Some artistic pictures were also made by Jos Leys. A popular view also appeared in [18], in La Recherche of April 1991 and also as cover of "Physik in unserer Zeit".

The most prominent application of these bearings in Nature seems to be shear bands as the one shown in Figure 3. Indeed rotations have been measured and simulated within shear bands in several occasions. Famous shear bands on a gigantic scale are faults between tectonic plates, like the San Andreas fault. They have so called "seismic gaps". i.e. regions without earthquakes or measurable

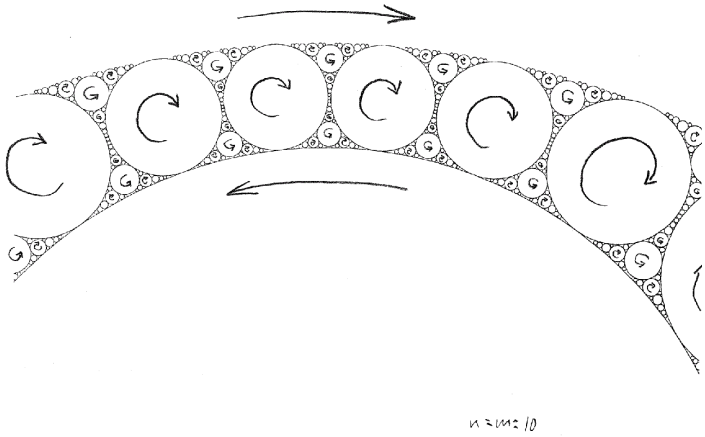

FIGURE 3

frictional heat. One way to measure rotations in geological faults is through the remnant magnetization of the earth as explained in [17]. That roller bearings do in fact spontaneously appear in shear bands has in fact also been observed in simulations of packings of disks of similar size under uniaxial load as we showed in a paper with Jan Åstrom and Jussi Timonen (see [3]). In [9] I combine this with the existence of three-dimensional bearings as discussed below.

Recently with Reza Mahmoodi we made some progress in three dimensions. We could construct five different topologies using conformal mappings as described in [11]. Together with Nick Rivier we could prove that in one case which is bichromatic (see Figure 4) it acts as a slip-free rolling, space-filling bearing as described in the paper published in [12] and as you can see in a movie. Jos Leys has produced beautiful pictures of our packings.

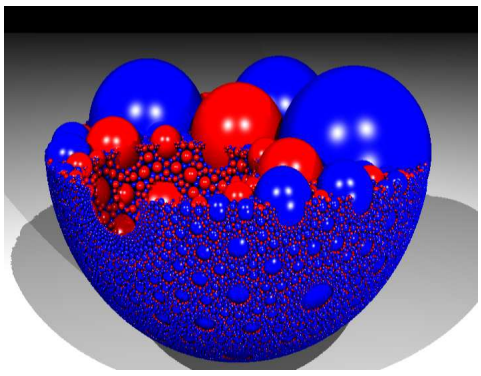

FIGURE 4

In Figure 4 one sees the new space-filling bearing based on an octahedron instead of a tetrahedron as usually used in Apollonian packings. Its fractal dimension is 2.58 as compared to 2.47 for the classical case. See also [8], or [4] and [15].

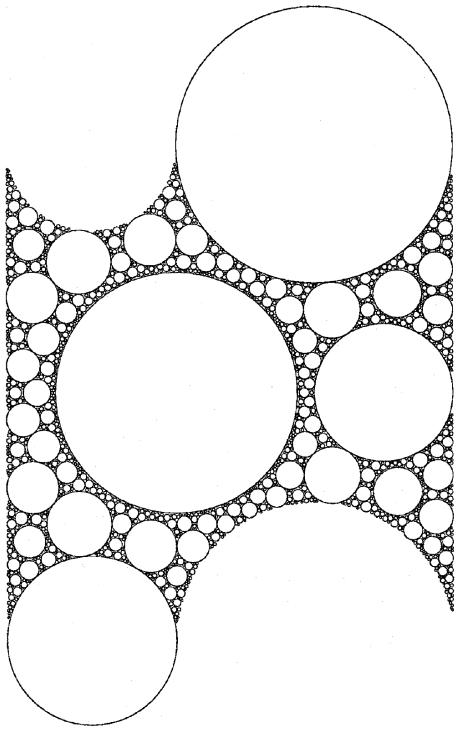

FIGURE 5

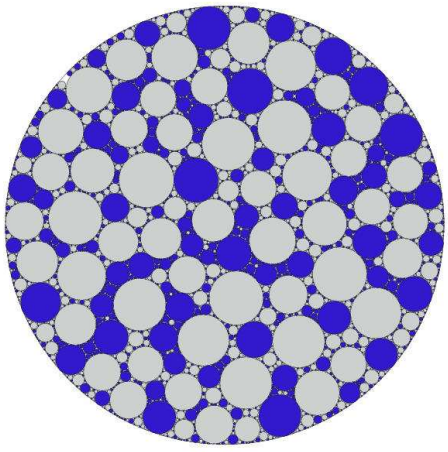

FIGURE 6

One up to now not really understood particularity of our conformal mapping method to construct self-similar packings is that in some specific cases of the second family of solutions the space is not completely filled but holes appear as seen in Figure 5. These holes are surrounded by a powder of infinitely small disks that

mechanically decouple the hole from the rest of the packing. Due to self similarity one never finds just one hole but if there is one hole there are also infinitely many smaller holes in the system.

As seen from Figure 6 it is also possible to construct random space-filling bearings. There blue circles only touch grey ones and grey only blue ones. At some places one might think that two blue do touch in the figure but in fact there is a layer of very small grey particles in between. This configuration is obtained numerically by placing one by one circles (or spheres) onto random positions into the not yet occupied space and repositioning and growing them until an even loop is created optimizing at the same time towards maximum filling (see [13]).

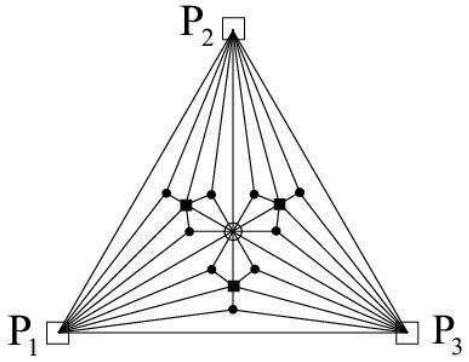

FIGURE 7

Finally I should mention that one can also study the network formed by the connections between the centers of mass of an Apollonian packing. We call them "Apollonian networks" (see Figure 7). They can be applied to porous media, polydisperse packings, road networks or electrical supply systems and they have interesting properties like being scale-free, ultrasmall world, Euclidean, matching and space-filling (see [2]). In fact this network already forms part of Wolfram's Mathematica .

A calculation of coupled maps on such a network has recently been achieved with Pedro Lind and Jason Gallas as can be seen in [10]. With Roberto Andrade we also wrote the extensive paper [1] on the properties of the ferro- and antiferromagnetic Ising model on the Apollonian network. All the links corresponding to this text are accessible from: http://www.comphys.ethz.ch/hans/appo.html

REFERENCES

[1] R.F.S. Andrade and H.J. Herrmann, *Magnetic models on Apollonian networks*, Phys. Rev. E **71** (2005), 0561311–0561318.

[2] J.S. Andrade, H.J. Herrmann, R.F.S. Andrade, and L.R. da Silva, *Apollonian Networks: Simultaneously Scale-Free, Small World, Euclidean, Space Filling, and with Matching Graphs*, Phys. Rev. Lett. **94** (2005), 0187021-0187024.

[3] J. A. Åström, H. J. Herrmann, and J. Timonen, *Granular Packings and Fault Zones*, Phys. Rev. Lett. **84** (2000), 638-641

[4] A. Cho, *One Good Turn Deserves Another*, Science Now (2004).
[5] H. J. Herrmann, G. Mantica, and D. Bessis , *Space-filling bearings*, Phys. Rev. Lett. **65** (1990), 3223-3226.
[6] H.J. Hermmann, *Space-filling Bearings*, Correlation and Connectivity in Physics and Biology, (Kluwer Academic Publishers, Dordrecht, 1990), 108–120
[7] H.J. Herrmann, *Les pavages d'engrenages*, Pour la Science **165** (1991), 17–18.
[8] H.J. Herrmann, R. Mahmoodi Baram, and M. Wackenhut, *Searching for the perfect packing*, Phys. A **330** (2003), 77–82.
[9] H.J. Herrmann, J.A. Åstrom and R. Mahmoodi Barama, *Rotations in shear bands and polydisperse packings*, Phys. A **344** (2004), 516–522.
[10] P.G. Lind, J.A.C. Gallas and H.J. Herrmann, *Coherence in scale-free networks of chaotic maps*, Phys. Rev. E **70** (2004), 0562071–056207.
[11] R. Mahmoodi Baram and H.J. Herrmann, *Self-similar space-lling packings in three dimensions*, Fractals, **12** (2004), 293–301.
[12] R. Mahmoodi Baram, H.J. Herrmann and N. Rivier, *Space-Filling Bearings in Three Dimensions*, Phys. Rev. Lett. **92** (2004), 0443011–0443014.
[13] R. Mahmoodi Baram, H.J. Herrmann, *Random Bearings and Their Stability*, Phys. Rev. Lett. **95** (2005), 2243031–2243034
[14] S.S. Manna, H.J. Herrmann, *Precise determination of the fractal dimensions of Apollonian packing and space-filling bearings*, J. Phys. A **24** (1991), L481–L490.
[15] J.R. Minkel *A Regal Bearing*, Scientific American, (April 2004).
[16] G. Oron, H.J. Herrmann *Generalization of space-filling bearings to arbitrary loop size* J. Phys. A **33** (2000). 1417–1434.
[17] S. Roux, A. Hansen, H.J. Herrmann, and J.P. Villote, *A model for gouge deformation: implications for remanent magnetization* Geophys. Res. Lett. **20** (1993), 1499–1502.
[18] P. Rodgers, *Fractal Bearings*, Physiscs World, (February, 1991).

Mechanics and growth of tissues

Jean-François Joanny
(joint work with M. Basan, J. Elgeti, F. Juelicher, J.Prost, J. Ranft, T. Risler)

Biological processes such as the growth of organs during development or the growth of a cancerous tumor involve tissue growth in which cell division overtakes cell death which is often due to apoptosis.

Research is this area has for a long time focused on genetic pathways that lead to gene regulation or genetic switches. It has however been realized recently that the mechanical properties of the tissue also plays an important role. The pattern of gene expression in a tissue can depend on the local stress as shown for example by perturbing the development of the fruit fly drosophila by applying external mechanical perturbations [1]. Similarly, during tumor growth, gene expression is coupled to the stress distribution inside the tumor and conversely the mechanical and the growth properties of the tumor depend on the gene expression pattern.

There is therefore an important interest to study the mechanics and growth of tissues. From a mechanical properties, a tissue is a complex system where elastic deformations and flows are coupled to the growth process. Two different approaches have been proposed. At the cell level, the tissue has been described as a foam-like structure which is constantly remodeled by cell division and cell

death [2]. The various phases obtained can be directly compared to observations of tissues during development.

We use here a more macroscopic approach based on a continuum mechanics which is valid at length scales larger than the cell size and at time scales longer than the cell division or apoptosis times [3]. This requires a constitutive equation for the tissue relating stress and deformation. Plant tissues are often considered as elastic solids. We argue here that both during cancer growth and development a tissue must be considered as a liquid or a visco-elastic fluid. Some tissues also have a yield stress and be considered as a plastic material.

We have recently proposed that the homeostatic pressure which is the pressure in the tissue in the steady state the cell division and death rates exactly balance be an important characteristic of the tissue. It could for example be one of the parameters giving information on the the invasiveness of the tissue. When two tissues are competing for the same space, we have shown that the tissue with the larger homeostatic pressure invades the tissue with the lower homeostatic pressure. Several experiments are currently being built in our laboratory to make systematic measurements of the homeostatic pressure.

An important feature of tissue growth is that cell division and cell death are coupled to the local stress. In many instances the axis of cell division is imposed by the principle axis of the stress acting on the cell. When this is taken into account in a tissue, the internal stresses generated by cell division and cell death relax the elastic stress in the tissue over a time scale which is proportional to the cell division time. Therefore, at a a time scale which is larger than the cell division or death time a tissue can be considered as a liquid with a viscosity or the order of the product of the cell elastic modulus and the cell division time. An important result is that close to the homeostatic state, not only the shear stress relaxes but also the isotropic component of the stress which relaxes to the negative of the homeostatic pressure. A tissue is thus a very unusual material which due to cell division and cell death is infinitely compressible and therefore can have large fluctuations. Examples of the liquid-like behavior of a tissue are given for the competition between two tissues and for the stability of the membrane between an epithelial tissue and a stroma.

An alternative way to study the mechanics and growth of tissues is to perform numerical simulations. We have built a simulation scheme based on the simulation method of liquids called 'Dissipative particle dynamics'. We introduced in this simulation scheme a very simple model for cell division and cell death. Although the results are only preliminary, they show that tissues indeed have a liquid-like behavior at timescales larger than the cell division time and they allow the calculation of the diffusion constant of a cell in the tissue. The diffusion constant increases linearly with the cell division rate in agreement with our theoretical description.

References

[1] E. Farge, *Mechanical Induction of Twist in the Drosophila Foregut/Stomodeal Primordium*, Current Biology **17** (2003), 1365–1377.

[2] R. Farhadifar et al., *The Influence of Cell Mechanics, Cell-Cell Interactions,and Proliferation on Epithelial Packing*, Current Biology **17** (2007), 2095–2104.
[3] M. Basan et al., *Homeostatic competition and its role in tumor growth and metastasis nucleation*, HFSP Journal **3** (2009), 265–272.

Active Matter: From Cells to Tissues

Frank Jülicher

One of the most fascinating features of living cells is their inherent dynamics. Dynamic cellular processes such as cell locomotion and cell division are driven on the molecular scale by active force generation in the cell cytoskeleton. The prototype for fore generation on the molecular scale are specialized motor molecules. Because of such active processes, the cytoskeleton becomes an active material which on large scales can be described by hydrodynamic equations. These hydrodynamic equations contain active terms describing for example active contributions to stresses in the material. In addition, if filaments of the cytoskeleton align locally this defines a local polar order which evolves dynamically. Active stresses become anisotropic if the material is polar. In that case spontaneous shear flows can be generated which in turn reorient filament polarity. Such active materials exhibit novel properties and are the basis to understand dynamics of cells but also on larger scales dynamic flows in tissues. a particular model system is the locomotion of cells on a solid substrate. This locomotion can be described as the consequence of active stresses in an anisotropic film on active fluid with specific boundary conditions describing local assembly and disassembly of filaments.

Mathematics of 2d Turbulence

Sergei Kuksin

For the purposes of this talk I assume that 2D turbulence is described by small-viscosity 2D Navier-Stokes equations (NSE), perturbed by a random force:

$$u'_t - \nu\Delta u + (u\cdot\nabla)u + \nabla p = \eta(t,x),$$

$$x\in\Gamma,\quad div\ u = 0\,;\quad 0<\nu\le 1.$$

Here $u(t,x)\in\mathbb{R}^2$ – velocity, $p(t,x)\in\mathbb{R}$ – pressure, $\eta(t,x)\in\mathbb{R}^2$ – random force. Γ is either a compact Rieman surface; e.g., $\Gamma = S^2$ or $\Gamma = \mathbb{T}^2 = \{(x_1,x_2)\mid 0\le x_1\le a,\ 0\le x_2\le b\}$. Or $\Gamma\Subset\mathbb{R}^2$ and $u\mid_{\partial\Gamma}=0$. For simplicity of notation assume that $\Gamma=\mathbb{T}^2$ or $\Gamma\Subset\mathbb{R}^2$. So $(u\cdot\nabla)u = u_1\frac{\partial}{\partial x_1}u + u_2\frac{\partial}{\partial x_2}u$.

Remarks. 1) Another way to introduce randomness in the Navier-Stokes equations would be through random initial data. For that model it is more difficult to get physically interesting results. I will not discuss it.

2) The random force in Navier-Stokes equations may be of the form

$\langle$ deterministic force $\rangle$ + $\langle$ small random perturbation $\rangle$.

Applying to the equation the Leray projection Π (see [1] or any mathematical book on NSE) and using that $\Pi\nabla p = 0$ and $\Pi u = u$, we write the Navier-Stokes equations as

$$u_t' - \nu Au + B(u) = \Pi\,\eta(t) =: \eta, \qquad (NSE)$$

where $Au = \Pi\Delta u$ and $B(u) = \Pi(u \cdot \nabla)u$.

Let $e_1, e_2, \dots$ be the basis of the space of divergence-free vector fields, satisfying the boundary conditions, formed by eigen-functions of A, $Ae_j = \lambda_j e_j \quad \forall\, j \geq 1$ (if $\Gamma = \mathbb{T}^2$, this the usual sin/cos basis).

The force η has the form $\eta(t,x) = \sum_j b_j \beta_j(t) e_j(x)$, where the constants $b_j \geq 0$ fast decay to zero and $\beta_j^\omega(t) = \frac{\partial}{\partial t} w_j(t) + f_j$, where $f_1, f_2, \dots$ are constants and $w_1(t), w_2(t), \dots$ are standard independent Wiener processes (we can handle another class of random forces, called *random kicks*. See in [1].

A solution $u(t)$ is a random Markov process in a function space. We are interested NOT in individual trajectories $t \mapsto u^\omega(t)$, but in distribution (=the law) of a solution $u(t)$. This is a probability measure μ_t in the function space, defined as follows: $\mu_t(Q) = \langle$probability that $(u(t) \in Q)\rangle$. We have $\mu_t = S_t^*(\mu_0)$, where $\{S_t^*\}$ is a semi-group of linear operators in the space of measures. The main task is to study qualitative properties of distributions of solutions, i.e. of the measures $\mu_t,\ t \geq 0$.

A measure μ in the function space is called a *stationary measure for (NSE)* if $S_t^*\mu \equiv \mu$. If $u(t)$ is a solution such that the law of $u(0) = \mu$, then the law of $u(t) \equiv \mu$. It is called a *stationary solution*. Existence of a stationary measure is an easy fact (it follows from compactness arguments). But its uniqueness is complicated.

Condition (C). $b_j > 0$ for each $j \leq N$, where $N = N(B_0, \nu, \Gamma)$.

For example, (C) holds if $b_j \neq 0$ for all j.

THEOREM 1 (see in [1]). If (C) holds, then:
1) there exists a unique stationary measure μ.
2) For any solution $u(t)$ of (NSE) the law $\mu(t)$ of this solution converges to μ exponentially fast (with respect to one of the 'usual' distances in the space of measures e.g., Prokhorov's or Wasserstein's).
3) If force $\eta(t,x)$ is smooth in x, then μ is supported by smooth functions.

So, "statistical properties of solutions for $t \gg 1$ are universal and are described by a unique stationary measure μ".

Theorem 1 has important consequences (see [1]):

THEOREM 2 (ergodicity). If (C) holds, then for any solution $u(t)$ of (NSE) and any 'good' $f(u)$ we have $\frac{1}{T}\int_0^T f(u(s))\,ds \to \langle \mu, f\rangle$, almost surely.

That is, "for a turbulent flow time-average equals ensemble-average".

THEOREM 3 (CLT). Let $\langle \mu, f\rangle = 0$. Then the law of $\frac{1}{\sqrt{T}}\int_0^T f(u(s))\,ds$ converges to a Gaussian measure $N(0,\sigma)$, for some $\sigma \geq 0$.

So "on large time-scales a turbulent flow is Gaussian".

Now let $\Gamma = \mathbb{T}^2$. 2d turbulence is described by solutions of (NSE) with $\nu \ll 1$. Consider the equation with small ν and with the force, multiplied by some degree of ν:

$$u'_t - \nu Au + B(u) = \nu^a \eta, \qquad a \in \mathbb{R}.$$

Solutions of this equation remain ~ 1 as $\nu \to 0$ if and only if $a = \frac{1}{2}$. Accordingly, below we discuss equation

$$u'_t - \nu Au + B(u) = \sqrt{\nu}\,\eta, \qquad 0 < \nu \le 1. \qquad (NSE_\nu)$$

Let (C) holds. Then eq. (NSE_ν) has a unique stationary measure μ_ν. Let $u_\nu(t,x)$ be the corresponding stationary solution. Assume that the force η is stationary in x. Then $u_\nu(t,x)$ is stationary both in t and in x. Also, $\mathrm{Re}\, u_\nu \sim \nu^{-1}$.

Task: study μ_ν and u_ν as $\nu \to 0$.

Theorem 4 (Eulerian Limit), see [1]. Every sequence $\nu'_j \to 0$ has a subsequence $\nu_j \to 0$ such that the law of the process $u_{\nu_j}(t,x)$ converges to the law of a process $U(t,x)$. This limiting process U is stationary in t and x. Moreover,
a) every its trajectory $U(t,x)$ as a function of x belongs to the Sobolev space H^2 and satisfies the free Euler equation

$$\dot u + (u\cdot\nabla)u + \nabla p = 0,\ \mathrm{d}iv\, u = 0. \qquad \text{(Eu)}$$

b) The energy $E(U) = \frac{1}{2}\|U(t)\|^2 = \frac{1}{2}\int |U(t,x)|^2\,dx$ is time-independent. If $g(\cdot)$ is a bounded continuous function, then $\int g(\mathrm{rot}\, U(t,x))\,dx$ also is time-independent.
c) the law μ_0 of $U(t)$ equals $\lim \mu_{\nu_j}$ and is an invariant measure for (Eu).
d) The measure μ_0 is such that the following integrals are finite and non-zero: $\int \|\nabla u\|^2\,\mu_0(du)$, $\int \|\Delta u\|^2\,\mu_0(du)$, $\int e^{\sigma\|\nabla u\|^2}\,\mu_0(du)$, for a suitable $\sigma > 0$.

μ_0 and $U(\cdot)$ are called the Eulerian limit for eq. (NSE_ν). They describe the space-periodic 2D turbulence since they describe solutions of (NSE) with $\nu \ll 1$ and $\mathrm{Re} \gg 1$.

Measure μ_0 is supported by Sobolev space H^2. If we write

$$u(x) = \sum_{s\in\mathbb{Z}^2} u_s\,\frac{s^\perp}{|s|}\,e^{is\cdot x}, \qquad E_s = \int |u_s|^2\mu_0(du), \quad s\in\mathbb{Z}^2.$$

then $\sum_{s\in\mathbb{Z}^2}|s|^2E_s = \int \|u\|^2_{H^2}\,\mu_0(du) < \infty$. I cannot prove a better estimate. (Numerics indicate that the relation above gives the right level of decay of E_s and $\sum |s|^{2+\varepsilon}E_s = \infty$ for $\varepsilon > 0$).

Now consider 3d NSE in the thin domain $(x_1,x_2,x_3) \in \Gamma\times(0,\varepsilon)$, perturbed by a random force. Assume free boundary conditions in the thin direction x_3: $u_3\ |_{x_3=0,\,\varepsilon} = 0$, $\partial_3 u_{1,2}\ |_{x_3=0,\,\varepsilon} = 0$. Then the law of $(u_1,u_2)(t,x_1,x_2,x_3)$ converges, as $\varepsilon\to 0$, to the law of a solution of randomly forced 2d NSE in Γ and we have

$$\mathbb{E}\,\langle\text{normalised energy of 3d flow}\rangle \to \mathbb{E}\,\langle\text{ energy of 2d flow}\rangle \qquad (*)$$

(so $\varepsilon^{-1}\int |u_3|^2\,dx \to 0$). It seems that (in non-trivial situations) $(*)$ does not hold for enstrophy, and that $\varepsilon^{-1}\int |\nabla u_3|^2\,dx$ does not converge to zero.

So randomly forced 2d NSE describe a class of anisotropic 3d turbulence. For these results for randomly forced 3d NSE see [2, 3]. Cf. well known related results for deterministic 3d NSE in thin domains due to G. Raugel, G. Sell and many people after them.

References

[1] S. Kuksin: *Randomly forced nonlinear PDEs and satistical hydrodynamics in 2 space dimensions*, 2006, European Math. Society.

[2] I. Chuyeshov and S. Kuksin in *ARMA* 188, 117-153 (2008).

[3] I. Chuyeshov and S. Kuksin in *Physica D* 237, 1352-1367 (2008).

On the relation of morphogenesis and non-Euclidean elasticity: scaling laws and thin film models

Marta Lewicka

The purpose of this note is to report on the recent development concerning thin film models for structures exhibiting residual stress at free equilibria. This phenomenon has been observed in different contexts: growing leaves, torn plastic sheets and specifically engineered polymer gels [7]. The study of wavy patterns in these contexts suggest that the sheet endeavors to reach a non-attainable equilibrium and hence assumes a non-zero stress rest configuration.

1. Elastic energy of a growing tissue. Consider a sequence of thin 3d films $\Omega^h = \Omega \times (-h/2, h/2)$, with an open, bounded and simply connected mid-plate $\Omega \subset \mathbb{R}^2$. Each Ω^h undergoes a growth process, described instanteneously by a given smooth tensor $a^h = [a^h_{ij}]$ with the property: $\det a^h(x) > 0$. According to the formalism in [15], the multiplicative decomposition $\nabla u = F a^h$ is postulated for the gradient of a deformation $u : \Omega^h \to \mathbb{R}^3$. The tensor $F = \nabla u (a^h)^{-1}$ corresponds to the elastic part of u, and accounts for the reorganization of Ω^h in response to the growth tensor a^h. The elastic energy of u depends hence only on F:

$$I^h_W(u) = \frac{1}{h} \int_{\Omega^h} W(\nabla u (a^h)^{-1}) \, \mathrm{d}x, \quad \forall u \in W^{1,2}(\Omega^h, \mathbb{R}^3). \tag{1}$$

The energy density $W : \mathbb{R}^{3\times 3} \longrightarrow \mathbb{R}_+$ is assumed to be $\mathcal{C}^2$ in a neighborhood of $SO(3)$, and to satisfy normalization, frame indifference and nondegeneracy:

$$\begin{aligned} \exists c > 0 \quad \forall F \in \mathbb{R}^{3\times 3} \quad \forall R \in SO(3) \quad & W(R) = 0, \quad W(RF) = W(F) \\ & W(F) \geq c \, \mathrm{dist}^2(F, SO(3)). \end{aligned} \tag{2}$$

2. Non-Euclidean elasticity. We now compare the above approach with the 'target metric' formalism [1, 12]. On each Ω^h we assume to be given a smooth Riemannian metric $g^h = [g^h_{ij}]$. A deformation u of Ω^h is an orientation preserving realization of g^h, when $(\nabla u)^T \nabla u = g^h$ and $\det \nabla u > 0$, or equivalently:

$$\nabla u(x) \in \mathcal{F}^h(x) = \Big\{ R\sqrt{g^h}(x); \; R \in SO(3) \Big\} \quad \text{a.e. in } \Omega^h. \tag{3}$$

It is hence instructive to study the following energy, bounding from below $I^h_W(u)$:

$$\tilde{I}^h_{dist}(u) = \frac{1}{h}\int_{\Omega^h} \mathrm{dist}^2(\nabla u(x), \mathcal{F}^h(x))\ \mathrm{d}x \qquad \forall u \in W^{1,2}(\Omega^h, \mathbb{R}^3), \tag{4}$$

and measuring the average pointwise deviation of u from orientation preserving realizations of g^h. Note that $\tilde{I}^h_{dist}$ is comparable in magnitude with I^h_W, for $W = \mathrm{dist}^2(\cdot, SO(3))$. Indeed, the intrinsic metric of the material is transformed by a^h to the target metric $g^h = (a^h)^T a^h$ and, for isotropic W, only the symmetric positive definite part of a^h given by $\sqrt{g^h}$ plays the role in determining the deformed shape.

We also consider a more general functional $\tilde{I}^h_W = \int W(x, \nabla u(x))$ with the inhomogeneous W satisfying frame invariance, normalisation and quadratic growth from below, as in (2) with respect to the energy well $\mathcal{F}^h$ given in (3).

3. Residual stress. Note that one could define the energy as the difference between the pull-back metric of a deformation u and the given metric: $I^h_{str}(u) = \int |(\nabla u)^T \nabla u - g^h|^2\ \mathrm{d}x$. However, such 'stretching' functional is not appropriate from the variational point of view, because there always exists $u \in W^{1,\infty}$ such that $I^h_{str}(u) = 0$. Further, if the Riemann curvature tensor R^h associated to g^h does not vanish identically, say $R^h_{ijkl}(x) \neq 0$, then u has a 'folding structure' [5]; it cannot be orientation preserving (or reversing) in any open neighborhood of x.

As proven in [12], the functionals I^h_W, $\tilde{I}^h_W$ and $\tilde{I}^h_{dist}$ have strictly positive infima for non-flat g^h, which points to the existence of non-zero stress at free equilibria (in the absence of external forces or boundary conditions):

$$R^h \not\equiv 0 \quad \Leftrightarrow \quad \inf\left\{\tilde{I}^h_{dist}(u);\ u \in W^{1,2}(\Omega^h, \mathbb{R}^3)\right\} > 0.$$

4. The prestrained Kirchhoff model. Several interesting questions arise in the study of the proposed energy functionals. A first one is to determine the scaling of the infimum energy in terms of the vanishing thickness $h \to 0$. Another is to find the limiting zero-thickness theories under obtained scaling laws.

In [12], we considered a first case where g^h is given by a tangential Riemannian metric $[g_{\alpha\beta}]$ on Ω, and is independent of the thickness variable. Consequently, if $[g_{\alpha\beta}]$ has non-zero Gaussian curvature $\kappa_{[g_{\alpha\beta}]}$, then each $R^h \not\equiv 0$. We proved that:

$$[g_{\alpha\beta}] \text{ has an isometric immersion } y \in W^{2,2}(\Omega, \mathbb{R}^3) \quad \Leftrightarrow \quad \inf \tilde{I}^h_{dist} \leq Ch^2,$$

It also follows that $\kappa_{[g_{\alpha\beta}]} \not\equiv 0$ iff $h^{-2} \inf \tilde{I}^h_{dist} \geq c > 0$. Existence of isometric immersions is a longstanding problem in differential geometry, depending heavily on the regularity [6]. We deal with $W^{2,2}$ immersions not studied previously.

More precisely, we prove that any sequence of deformations u^h with $\tilde{I}^h_W(u^h) \leq Ch^2$, converges to an isometric immersion y as above. Conversly, every y can be recovered as a limit of u^h whose energy scales like h^2. The Γ-limit of the energies is a curvature functional on the space of all $W^{2,2}$ realizations y of $[g_{\alpha\beta}]$ in $\mathbb{R}^3$:

$$\frac{1}{h^2}\tilde{I}^h_W \xrightarrow{\ \Gamma\ } \frac{1}{24}\int_\Omega \mathcal{Q}_2(x')\Big(\sqrt{[g_{\alpha\beta}]}^{-1}(\nabla y)^T \nabla \vec{n}\Big)\ \mathrm{d}x',$$

Here $\vec{n}$ is the unit normal to the surface $y(\Omega)$, while $\mathcal{Q}_2(x')$ are the quadratic forms, nondegenerate and positive definite on the symmetric 2×2 tensors, which can be calculated explicitely (see [12]) from $\nabla^2 W(x', \sqrt{[g_{\alpha\beta}]})$.

5. Rigidity estimate. As a ingredient of proofs, we give a generalization of [3] to the non-Euclidean setting. For all $u \in W^{1,2}(\mathcal{U}, \mathbb{R}^n)$ there exists $Q \in \mathbb{R}^{n\times n}$:

$$\int_{\mathcal{U}} |\nabla u(x) - Q|^2 \, \mathrm{d}x \leq C \left(\int_{\mathcal{U}} \mathrm{dist}^2(\nabla u, \mathcal{F}(x)) \, \mathrm{d}x + \|\nabla g\|^2_{L^\infty} (\mathrm{diam}\, \mathcal{U})^2 |\mathcal{U}| \right),$$

where $\mathcal{F}$ is the energy well as in (3) relative to given metric g on $\mathcal{U}$. The constant C depends on $\|g\|_{L^\infty}$, $\|g^{-1}\|_{L^\infty}$, and on $\mathcal{U}$, uniformly for a family of domains which are bilipschitz equivalent with controlled Lipschitz constants.

6. The prestrained von Kármán model. Towards studying the dynamical growth problem, in [8] we considered the growth tensor of the form:

$$a^h(x', x_3) = \mathrm{Id} + h^2 \epsilon_g(x') + h x_3 \gamma_g(x'),$$

with given matrix fields $\epsilon_g, \gamma_g : \overline{\Omega} \to \mathbb{R}^{3\times 3}$. We proved that $\inf I^h_W \leq Ch^4$, while the lower bound $h^{-4} \inf I^h_W \geq c > 0$ is equivalent to:

$$\mathrm{curl}((\gamma_g)_{tan}) \not\equiv 0 \qquad \text{or} \qquad 2\mathrm{curl}^T \mathrm{curl}(\epsilon_g)_{tan} + \det(\gamma_g)_{tan} \not\equiv 0,$$

which are the (negated) linearized Gauss-Codazzi equations corresponding to the metric $I = \mathrm{Id} + h^2(\epsilon_g)_{tan}$ and the second fundamental form $II = \frac{1}{2} h (\gamma_g)_{tan}$ on Ω.

The Γ-limit of the rescaled energies is now expresed in terms of the out-of-plane displacement $v \in W^{2,2}(\Omega, \mathbb{R})$ and in-plane displacement $w \in W^{1,2}(\Omega, \mathbb{R}^2)$:

$$\frac{1}{h^4} I^h_W \xrightarrow{\Gamma} \frac{1}{24} \int_\Omega \mathcal{Q}_2\big(\nabla^2 v + \frac{1}{2}(\gamma_g)_{tan}\big) + \frac{1}{2} \int_\Omega \mathcal{Q}_2\big(\mathrm{sym}\nabla w + \frac{1}{2} \nabla v \otimes \nabla v - \frac{1}{2}(\epsilon_g)_{tan}\big).$$

The two terms above measure: the first order in h change of II, and the second order change in I, under the deformation $id + hve_3 + h^2 w$ of Ω. Moreover, any sequence of deformations u^h with $I^h_W(u^h) \leq Ch^4$ is, asymptotically, of this form.

For W isotropic, the Euler-Lagrange equations of the limiting functional are equivalent, under a change of variables which replaces the in-plane displacement w by the Airy stress potential Φ, the system proposed in [14]:

$$\Delta^2 \Phi = -S(K_G + \lambda_g), \qquad B\Delta^2 v = [v, \Phi] - B\Omega_g, \tag{5}$$

with S the Young's modulus, K_G the Gaussian curvature, B the bending stiffness, and $\nu = \lambda/(2(\lambda+\mu))$ the Poisson ratio given in terms of the Lamé constants λ and μ. The corrections due to the prestrain are: $\lambda_g = \mathrm{curl}^T \mathrm{curl}\ (\epsilon_g)_{2\times 2}$ and $\Omega_g = \mathrm{div}^T \mathrm{div}\ ((\gamma_g)_{2\times 2} + \nu\ \mathrm{cof}\ (\kappa_g)_{2\times 2})$. When $\mathcal{Q}_2 = \mathrm{Id}$, (5) has the form:

$$\Delta^2 \Phi = -\det \nabla^2 v - \frac{1}{2} \mathrm{curl}^T \mathrm{curl}(\epsilon_g)_{tan}, \quad \Delta^2 v = 12\, \mathrm{cof}\nabla^2 \Phi : \nabla^2 v - \frac{1}{2} \mathrm{div}^T \mathrm{div}(\gamma_g)_{tan}.$$

7. A hierarchy of scalings. We expect it should be possible to rigorously derive a hierarchy of prestrained limiting theories, differentiated by the embeddability properties of the target metrics. This is in the same spirit as the different scalings of external forces lead to a hierarchy of nonlinear elastic plate theories recently displayed by Friesecke, James and Müller [4]. For shells, that are thin

films with mid-surface or arbitrary (non-flat) geometry, an infinite hierarchy of models was proposed, by means of asymptotic expansion in [13], and it remains in agreement with all the rigorously obtained results [2, 9, 10, 11].

Acknowledgements. Supported by grants NSF DMS-0707275 and DMS-0846996.

References

[1] E. Efrati, E. Sharon and R. Kupferman, *Elastic theory of unconstrained non-Euclidean plates*, J. Mechanics and Physics of Solids, **57** (2009), 762–775.

[2] G. Friesecke, R. James, M.G. Mora and S. Müller, *Derivation of nonlinear bending theory for shells from three-dimensional nonlinear elasticity by Gamma-convergence*, C. R. Math. Acad. Sci. Paris, **336** (2003), no. 8, 697–702.

[3] G. Friesecke, R. James and S. Müller, *A theorem on geometric rigidity and the derivation of nonlinear plate theory from three dimensional elasticity*, Comm. Pure. Appl. Math., **55** (2002), 1461–1506.

[4] G. Friesecke, R. James and S. Müller, *A hierarchy of plate models derived from nonlinear elasticity by gamma-convergence*, Arch. Ration. Mech. Anal., **180** (2006), no. 2, 183–236.

[5] M. Gromov, *Partial Differential Relations*, Springer-Verlag, Berin-Heidelberg, (1986).

[6] Q. Han and J.-X. Hong, *Isometric embedding of Riemannian manifolds in Euclidean spaces*, Mathematical Surveys and Monographs, **130** AMS, Providence, RI (2006).

[7] Y. Klein, E. Efrati and E. Sharon, *Shaping of elastic sheets by prescription of non-Euclidean metrics*, Science, **315** (2007), 1116–1120.

[8] M. Lewicka, L. Mahadevan and M.R. Pakzad, *Morphogenesis of growing elastic tissues: the rigorous derivation of von Kármán equations with residual stress*, submitted.

[9] M. Lewicka, M.G. Mora and M.R. Pakzad, *Shell theories arising as low energy Γ-limit of 3d nonlinear elasticity*, to appear in Ann. Scuola Norm. Sup. Pisa Cl. Sci. (2009).

[10] M. Lewicka, M.G. Mora and M.R. Pakzad, *A nonlinear theory for shells with slowly varying thickness*, C.R. Acad. Sci. Paris, Ser I **347** (2009), 211–216

[11] M. Lewicka, M.G. Mora and M.R. Pakzad, *The matching property of infinitesimal isometries on elliptic surfaces and elasticity of thin shells*, submitted (2008).

[12] M. Lewicka and M.R. Pakzad, *Scaling laws for non-Euclidean plates and the $W^{2,2}$ isometric immersions of Riemannian metrics*, submitted (2009).

[13] M. Lewicka and M.R. Pakzad, *The infinite hierarchy of elastic shell models; some recent results and a conjecture*, submitted (2009).

[14] L. Mahadevan and H. Liang, *The shape of a long leaf*, Proc. Nat. Acad. Sci. (2009).

[15] E.K. Rodriguez, A. Hoger and A. McCulloch, J.Biomechanics **27**, 455 (1994).

Vanishing-viscosity solutions for rate-independent systems

Alexander Mielke

In these notes we give an overview of the recently developed theory for rate-independent systems. Such systems are used to model hysteresis, dry friction, elastoplasticity, magnetism, and phase transformation, and they are characterized by the fact that the changes of the state are driven solely by changes of the loading.

General energy-driven systems, also called generalized gradient systems, are characterized by a triple $(\boldsymbol{Z}, \mathcal{I}, \mathcal{R})$ where the Banach space $\boldsymbol{Z}$ is the state space and $\mathcal{I} : [0,T] \times \boldsymbol{Z} \to \mathbb{R}_\infty := \mathbb{R} \cup \{\infty\}$ is the energy functional. The dissipation potential $\mathcal{R} : \boldsymbol{Z} \times \boldsymbol{Z} \to [0,\infty]$ allows us to write the evolution equation in the form

$$0 \in \partial_{\dot z} \mathcal{R}(z, \dot z) + \overline{\partial}_z \mathcal{I}(t, z) \quad \subset \boldsymbol{Z}^*, \tag{1}$$

where $\overline{\partial}_z$ denotes a suitable subgradient of $\mathcal{I}(t,\cdot)$, while $\partial_{\dot z}\mathcal{R}(z,\cdot)$ denotes the convex subdifferential of $\mathcal{R}(z,\cdot)$. The generalized gradient system $(\boldsymbol{Z},\mathcal{I},\mathcal{R})$ is rate independent if $\mathcal{R}(z,\cdot)$ is positively homogeneous of degree 1, since this implies $\partial_v\mathcal{R}(z,\alpha v)=\partial_v\mathcal{R}(z,v)$ for all $\alpha>0$. We then call $(\boldsymbol{Z},\mathcal{I},\mathcal{R})$ a rate-independent system, shortly RIS. Hence, system (1) is necessarily nonsmooth. In fact, the convex subdifferential $\partial_v\mathcal{R}(z,\cdot):\boldsymbol{Z}\rightrightarrows\boldsymbol{Z}^*$ is not continuous and set-valued.

However, the main difference to the usually studied generalized gradient flows is that $\mathcal{R}(z,\cdot)$ has at most linear growth, and we cannot guarantee continuity of the solutions $z:[0,T]\to\boldsymbol{Z}$. Since we can guarantee the absolute continuity needed in (1) only under strong convexity assumptions (cf. [MiR07], we mainly discuss the question, how the strong differential form should be weakened to allow for solutions with jumps. For full details we refer to the survey [Mie09] or the papers [MRS09b, MRS09a, MiZ09].

To motivate the main structures of the different solution concepts for RIS, we start from the Fenchel equivalence ($\mathcal{R}^*(z,\cdot)$ is the Legendre transform of $\mathcal{R}(z,\cdot)$)

$$\eta\in\partial_v\mathcal{R}(z,v)\quad\Longleftrightarrow\quad v\in\partial_\eta\mathcal{R}^*(z,\eta)\quad\Longleftrightarrow\quad\mathcal{R}(z,v)+\mathcal{R}^*(z,\eta)\le\langle\eta,v\rangle.$$

While the statement on the left-hand side of this equivalence is a force balance, the statement on the right-hand side is given in terms of energy rates. Using $-\eta=\xi(t)\in\overline{\partial}_z\mathcal{I}(t,z(t))$ and a chain rule, we find that (1) is equivalent to the scalar, upper energetic inequality

$$\begin{aligned}\mathcal{I}(T,z(T))+\textstyle\int_0^T\mathcal{R}(z(t),\dot z(t))+\mathcal{R}^*(z(t),-\xi(t))\,\mathrm{d}t\\ \le\mathcal{I}(0,z(0))+\textstyle\int_0^T\partial_t\mathcal{I}(t,z(t))\,\mathrm{d}t.\end{aligned}\tag{2}$$

The particularity of RIS is that $\mathcal{R}^*(z,-\xi)$ only takes the two values 0 and ∞, viz. $\mathcal{R}^*(z,-\xi)=0$ if and only if $0\in\partial_v\mathcal{R}(z,0)+\xi$. Thus, the energetic inequality (2) can be rewritten in terms of two conditions

$$\text{(3a)}\qquad\text{local stability}\qquad 0\in\partial_v\mathcal{R}(z(t),0)+\overline{\partial}_z\mathcal{I}(T,z(t))\ \text{a.e. in }[0,T],$$

$$\text{(3b)}\qquad\text{energy inequality}\qquad\begin{aligned}&\mathcal{I}(T,z(T))+\mathrm{Diss}_{\mathcal{R}}(z,[0,T])\\ &\qquad\le\mathcal{I}(0,z(0))+\textstyle\int_0^T\partial_t\mathcal{I}(t,z(t))\,\mathrm{d}t,\end{aligned}$$

where $\mathrm{Diss}_{\mathcal{R}}(z,[r,t])=\int_r^t\mathcal{R}(z(s),\dot z(s))\,\mathrm{d}s$ is the energy dissipated in $[r,t]$.

The local stability condition is a purely static concept and does not involve any time dependence, which shows that RIS are very close to static systems. Relation (3b) is a simple scalar energy inequality, which in fact should hold as an identity and also for all times $t\in[0,T]$ and not just for $t=T$. In all the different solution concepts discussed below we have these two different principles, namely (i) a static stability condition and (ii) an energy inequality. However, a crucial point in the definitions of solutions to RIS is always that the stability condition and the energy inequality interact in such a way that the stability condition implies a lower energy estimate on all subintervals of $[0,T]$, which together with the upper energy estimate (3b) provides energy balance on all subintervals.

Local solutions were introduced in [ToZ09] and are characterized by (3a) and the upper energy estimate (3b) but for each subinterval $[r,t] \subset [0,T]$. This notion is still quite general and all solutions consider here fall into this class.

Energetic solutions (also called *irreversible quasistatic evolutions* in [DaT02, DFT05], and surveyed in [Mie05]) ask for an energy equality (E), where the dissipation is formulated in terms of a dissipation distance $\mathcal{D} : \boldsymbol{Z} \times \boldsymbol{Z} \to [0,\infty]$. Moreover, the local stability (3a) is replaced by a global stability conditions (S), namely $\mathcal{I}(t,z(t)) \le \mathcal{I}(t,\widetilde{z}) + \mathcal{D}(z(t),\widetilde{z})$ for all $\widetilde{z} \in \boldsymbol{Z}$.

Parametrized solutions are obtained in the vanishing-viscosity limit in

$$0 \in \partial_{\dot z}\mathcal{R}(z^\varepsilon,\dot z^\varepsilon) + \varepsilon \mathbb{V}\dot z^\varepsilon + \overline{\partial}_z \mathcal{I}(t,z^\varepsilon) \quad \subset \boldsymbol{Z}^*, \tag{4}$$

after an arclength parametrization. Taking the limit $\varepsilon \to 0$ directly in $z^\varepsilon : [0,T] \to \boldsymbol{Z}$ is difficult because of the formation of jumps, i.e. fast transitions on time intervals of length $1/\varepsilon$. We use the arclength parametrization $\zeta^\varepsilon = (\tau_\varepsilon, Z_\varepsilon) : [0,S^\varepsilon] \to \mathbb{R} \times \boldsymbol{Z}$ such that $\tau_\varepsilon'(s) + \|Z_\varepsilon'(s)\|_{\mathbb{V}} = 1$ and $z^\varepsilon(\tau_\varepsilon(s)) = Z_\varepsilon(s)$ a.e. The limit $\zeta = (t,Z)$ for $\varepsilon \to 0$ is called parametrized solution and satisfies the limit problem

$$0 \in \partial_{\dot Z}\mathcal{R}(Z(s),Z'(s)) + \partial\mathcal{C}(Z'(s)) + \overline{\partial}_Z \mathcal{I}(\tau(s),Z(s)), \quad \tau'(s) + \|Z'(s)\|_{\mathbb{V}} = 1,$$

where $\mathcal{C}(v) = 0$ for $\|v\|_{\mathbb{V}} = \langle \mathbb{V}v, v\rangle^{1/2} \le 1$ and ∞ otherwise. Existence results for parabolic situations are established in [MiZ09].

BV solutions $\widetilde{z} : [0,T] \to Z$ are in principle defined as projections of the parametrized solutions, i.e. there exists a parametrized solution $\zeta = (\tau, Z)$ such that $(t,\widetilde{z}(t)) = (\tau(s(t)), Z(s(t))$ for some monotone $s : [0,T] \to [0,S]$. However, it is important to have an independent characterization which can be obtained via the *vanishing-viscosity contact potential*

$$\boldsymbol{p}(v,\xi) := \inf\big\{\, \mathcal{R}_\varepsilon(v) + \mathcal{R}_\varepsilon^*(\xi) \,\big|\, \varepsilon > 0 \,\big\} \text{ with } \mathcal{R}_\varepsilon(v) = \Psi(v) + \frac{\varepsilon}{2}\langle \mathbb{V}v, v\rangle.$$

This allows us to define a supplemented dissipation distance via

$$\Delta(t,z_0,z_1) := \inf\big\{ \textstyle\int_{r=0}^1 \boldsymbol{p}(\dot y(r), -\mathrm{D}\mathcal{I}(t,y(r)))\,\mathrm{d}r \;\big|\; y \in \mathrm{W}^{1,1}([0,1];\boldsymbol{Z}),\ y(0)=z_0,\ y(1)=z_1\big\}.$$

Note that $\Delta(t,z_0,z_1) \ge \Psi(z_1-z_0) \ge \|z_1-z_0\|_{\boldsymbol{X}}$ for some Banach space $\boldsymbol{X}$.

A function $\widetilde{z} : [0,T] \to \boldsymbol{Z}$ is called a *BV solution* of the RIS $(\boldsymbol{Z},\mathcal{I},\Psi,\mathbb{V})$, if $\widetilde{z} \in \mathrm{BV}([0,T];\boldsymbol{X}) \cap \mathrm{L}^\infty([0,T];\boldsymbol{Z})$ and the following holds:

(5a) local stability $\quad \forall\, t \in C(z) :\ 0 \in \partial\Psi(0) + \overline{\partial}_z \mathcal{I}(t,z)$;

(5b) energy balance
$\forall\, t \in [0,T]$: $\mathcal{I}(t,z(t)) + \mathrm{Diss}_{\boldsymbol{p},\mathcal{I}}(z,[0,t]) = \mathcal{I}(0,z(0)) + \int_0^t \partial_\tau \mathcal{I}(\tau,z(\tau))\,\mathrm{d}\tau$,

where $C(\widetilde{z}) \subset [0,T]$ denotes the continuity points of $\widetilde{z} : [0,T] \to \boldsymbol{X}$ and $\mathrm{Diss}_{\boldsymbol{p},\mathcal{I}}$ is a special variation of defined via Ψ at continuity points and Δ at jump points, see [MRS09a, Mie09]. These works contain first convergence results of the viscous

approximations z^ε towards BV solutions. Moreover, for viscous time-incremental problems of the form

$$z_k^{\varepsilon,\delta} \ \in \ \mathrm{Argmin}\, \mathcal{I}(k\delta, z) + \delta \mathcal{R}_\varepsilon\Big(\frac{1}{\delta}(z - z_{k-1}^{\varepsilon,\delta})\Big),$$

where $\delta > 0$ is the time-step, it is shown that the piecewise affine interpolants $\widehat{z}^{\varepsilon,\delta} : [0,T] \to \boldsymbol{Z}$ converge to BV solutions if ε, δ, and δ/ε tend to 0. If instead, ε/δ goes to 0, then the limits are energetic solutions.

Acknowledgments. The research was partially supported by DFG via Research Unit 787 *MicroPlast* (Project Mie 459/5) and partially co-authored by Riccarda Rossi, Giuseppe Savaré, and Sergey Zelik.

References

[DaT02] G. Dal Maso and R. Toader. A model for quasi–static growth of brittle fractures: existence and approximation results. *Arch. Rational Mech. Anal.*, 162, 101–135, 2002.

[DFT05] G. Dal Maso, G. Francfort, and R. Toader. Quasistatic crack growth in nonlinear elasticity. *Arch. Rational Mech. Anal.*, 176, 165–225, 2005.

[Mie05] A. Mielke. Evolution in rate-independent systems (Ch. 6). In C. Dafermos and E. Feireisl, editors, *Handbook of Differential Equations, Evolutionary Equations, vol. 2*, pages 461–559. Elsevier B.V., Amsterdam, 2005.

[Mie09] A. Mielke. *Differential, energetic and metric formulations for rate-independent processes.* WIAS preprint 1454, 2009. C.I.M.E. Springer Lecture Notes. To appear.

[MiR07] A. Mielke and R. Rossi. Existence and uniqueness results for a class of rate-independent hysteresis problems. *Math. Models Meth. Appl. Sci.*, 17, 81–123, 2007.

[MiZ09] A. Mielke and S. Zelik. On the vanishing viscosity limit in parabolic systems with rate-independent dissipation terms. *In preparation*, 2009.

[MRS09a] A. Mielke, R. Rossi, and G. Savaré. BV solutions and viscosity approximations of rate-independent systems. *ESAIM Control Optim. Calc. Var.*, October 2009. Submitted. WIAS preprint 1451.

[MRS09b] A. Mielke, R. Rossi, and G. Savaré. Modeling solutions with jumps for rate-independent systems on metric spaces. *Discr. Cont. Dynam. Systems Ser. A*, 25(2), 585–615, 2009.

[ToZ09] R. Toader and C. Zanini. An artificial viscosity approach to quasistatic crack growth. *Boll. Unione Matem. Ital.*, 2(1), 1–36, 2009.

On a mesoscopic many-body Hamiltonian describing elastic shears and dislocations

Luca Mugnai

(joint work with Stephan Luckhaus)

We assume that low-energy states in a mono-atomic crystalline material are given by approximately linear deformations of a ground state lattice (here a simple Bravais-lattice $\mathcal{L}_G := \{Gz : \ z \in \mathbb{Z}^d\}$, for some $G \in GL^+(d, \mathbb{R})$). Hence we construct a "mesoscopic" many-body interaction potential acting on finite systems of particles (a Hamiltonian in the language of statistical mechanics and of this report) that is able to describe deformed crystals with defects. More precisley the

Hamiltonian we present measures the shear and the deviations from the linearly sheared ground-state lattice in a mesoscopic interaction range.

In order to describe the construction of the Hamiltonian and its relation to measurable quantities, we need to introduce some notation. With Ω we denote an open, connected, bounded, subset of $\mathbb{R}^d$ ($d \leq 3$), and with $\mathcal{X} := \{x_i\}_{i\in I} \subset \Omega$ we denote a finite subset whose elements represent the positions of the particles of a given configuration. We define the Hamiltonian in two steps. In the first step we define an "energy density" which depends on: the point $x \in \Omega$ in the Eulerian space; an auxiliary variable represented by an affine deformation; and the particle configuration $\mathcal{X}$ in a finite neighborhood (range) of x of size $\lambda << L$ ($L > 0$ being the diameter of Ω). In the second step we integrate the "energy-density" over the Eulerian coordinate $x \in \Omega$ and minimize it with respect to the affine deformation. As a result we obtain a Hamiltonian which depends only on the particle configuration and, in our case, is invariant with respect to rigid motions and permutations acting on $\mathcal{X}$.

Let us describe in more detail how the Hamiltonian is constructed. For a point $x \in \Omega$, an affine map $(A, \tau) \in GL^+(d, \mathbb{R}) \times \mathbb{R}^d$ and the finite particle configuration $\mathcal{X}$, our "energy-density" is given by the sum of three terms:

(i) The first term is obtained assignin a value to the linearly deformed ground-state lattice $\mathcal{L}(A) := \{Az : z \in \mathbb{Z}^d\}$;

(ii) The second term is obtained assignin an excess-energy for each individual particle $x_i \in \mathcal{X}$ through a periodic potential which has the periodicity of the lattice $\mathcal{L}_x(A, \tau) := \{A(z-\tau)+x : z \in \mathbb{Z}^d\}$, and which can be thought as a one-particle potential in an otherwise periodic lattice, multiplied with a cut-off function of finite mass to ensure a finite interaction range;

(iii) The third and last term penalizes the presence of "vacancies" measuring the difference between the determinant of the inverse of the deformation A and the empirical density of a point.

The analytical expression of the term described in (i) is given by a function $F \in C^2(GL^+(d, \mathbb{R}), [0, +\infty))$ such that

- $F(A) \geq 0$ for every $A \in GL^+(d, \mathbb{R})$;
- F is frame-indifferent, that is $F(RA) = F(A)$ for every rotation R acting on $\mathbb{R}^d$;
- F is invaraint with respect to (positive) changes of the lattice-basis of $\mathcal{L}(A)$, that is $F(A) = F(AB)$ for every $B \in \mathbb{Z}^{d\times d}$ such that $\det B = 1$;
- the function F takes its minum on the ground-state lattice $\mathcal{L}_G$. That is

$$\{F = 0\} = \{\widetilde{G} \in GL^+(d, \mathbb{R}) : \mathcal{L}(\widetilde{G}) = \mathcal{L}(G)\}.$$

The analytical expression of the second term, the one described in (ii) above, is

$$\frac{1}{\lambda^d} \sum_{x_i \in I} \Big[W\big(x_i,\, \mathcal{L}_x(A, \tau)\big) - \vartheta_0 \Big] \varphi_{\lambda,x}(x_i),$$

where: for fixed $x \in \Omega$ and $(A, \tau) \in GL^+(d, \mathbb{R}) \times \mathbb{R}^d$, the function $W : \mathbb{R}^d \times GL^+(d, \mathbb{R}) \times \mathbb{R}^d \to [0, +\infty)$ behaves similarly to the squared-distance from the

lattice $\mathcal{L}_x(A,\tau)$; $\vartheta_0 > 0$ is a positive constant; and $\varphi_{\lambda,x}(\cdot) \in C^\infty(\mathbb{R}^d, [0,1])$ is a cut-off function supported in the ball of radius 2λ centered at x, with finite mass independent of x. The last term, corresponding to (iii), is given by

$$\vartheta_1 \Big(\frac{1}{\det A} - \frac{1}{C_\varphi \, \lambda^d} \sum_{x_i \in \mathcal{X}} \varphi_{\lambda,x}(x_i) \Big),$$

where $\vartheta_1 > 0$ is a constant, and C_φ is a renormalizing factor depending on the cut-off function $\varphi_{\lambda,x}$. Finally we define the energy density at a point x, depending still on the auxiliary variable represented by the affine deformation $\mathcal{A} = (A,\tau) \in GL^+(d,\mathbb{R}) \times \mathbb{R}^d$, as follows

$$\begin{aligned} h_\lambda(x,\mathcal{A},\mathcal{X}) :=& F(A) + \frac{1}{\lambda^d} \sum_{x_i \in I} \Big[W\big(x_i,\, \mathcal{L}_x(A,\tau)\big) - \vartheta_0 \Big] \varphi_{\lambda,x}(x_i) \\ &+ \vartheta_1 \Big(\frac{1}{\det A} - \frac{1}{C_\varphi \, \lambda^d} \sum_{x_i \in \mathcal{X}} \varphi_{\lambda,x}(x_i) \Big). \end{aligned}$$

Note that the third term can be incorporated in the first two, but its meaning is the cost of a vacancy. As we already said $W(\cdot, \mathcal{L}_x(A,\tau))$ has the period of the affinely deformed ground-state lattice $\mathcal{L}_x(A,\tau)$. The meaning of $-\vartheta_0$ is that of the energy per particle in the ground-state, $D^2_{yy} W(0, \mathcal{L}_x(A,\tau))$ is the quadratic-form describing independent deviations of particles from the lattice position, and $F(A)$ the energy-cost of a linear deformation of the ground-state lattice. Eventually we define the Hamiltonian

$$H_\lambda(\mathcal{X},\Omega) := \int_\Omega \Big[\inf_{\mathcal{A} \in GL^+(d,\mathbb{R}) \times \mathbb{R}^d} h_\lambda(x,\mathcal{A},\mathcal{X}) \Big] \, dx.$$

Minimization of $h_\lambda(x,\mathcal{A},\mathcal{X})$ with respect to $\mathcal{A}$ is approximately the same as identifying the optimally fitted lattice, and then calculating its energy $F(A)$ plus the cost of the deviation from this lattice. As a consequence we deduce that the Hamiltonian can give a "realistic" picture only for low energy states.

In fact the results we obtained in [5] contribute to the descriptions of low energy states. More precisely we consider low-energy configurations with an additional hard-core constraint, and an uniform lower bound on the empirical density. The result we are able to prove is that low-energy configurations are characterised by a large set of low energy-density whose connected components we call "grains". On each open, simply connected subset U of a grain we show the existence of a family of maps $\mathcal{A}_\mathcal{B} = (A_\mathcal{B}, \tau_\mathcal{B}) \in C^1(U,\, GL^+(d,\mathbb{R}) \times \mathbb{R}^d)$ indexed by $\mathcal{B} \in GL^+(d,\mathbb{Z}) \times \mathbb{Z}^d$ (the set of affine maps leaving a simple Bravais-lattice invariant) with the following properties. For every $x \in U$ we have

$$h_\lambda(x, \mathcal{A}_\mathcal{B}(x), \mathcal{X}) = \inf_{\mathcal{A} \in GL^+(d,\mathbb{R}) \times \mathbb{R}^d} h_\lambda(x,\mathcal{A},\mathcal{X}).$$

Moreover

$$\lambda \|\nabla A_\mathcal{B}(\cdot)\|_{L^\infty(U)} + \|\nabla \tau_\mathcal{B}(\cdot) - A_\mathcal{B}^{-1}(\cdot)\|_{L^\infty(U)} \le \frac{C^\mathcal{B}_\nabla}{\lambda},$$

where $C^{\mathcal{B}}_{\nabla} > 0$ is a constant which is proportional to the "small" value of $h_\lambda(x, \mathcal{A}_{\mathcal{B}}(x), \mathcal{X})$. Moreover we can think of the shift part of the affine deformation $\tau_{\mathcal{B}}$ as a transformation from Eulerian to Lagrangian coordinates, while we can think of its inverse as the (local) deformation which is defined only up to the period of the lattice (e.g. the flat torus). If a grain is not simply connected it can happen that going around a closed curve one ends up with a vector in the lattice corresponding to a "jump" in $\tau_{\mathcal{B}}$. In this case we say that the loop wraps around a dislocation and we call the lattice-vector the Burgers vector associated with the dislocation.

If one wants to be very precise in algebraic terms, in this theory a dislocation structure (in a grain) is a homeomorphism from the homothopy group of the grain into $GL^+(d, \mathbb{Z}) \times \mathbb{Z}^d$, only it turns out that a nontrivial component in $GL^+(d, Z)$ is much more costly in energy than one in $\mathbb{Z}^d$ (the Burgers vector).

Note that much of the final description is very similar to the one given in a rational mechanics context by Kondo [3] and Kröner [4] (see also [2]). However our purpose is to make the connection with a Hamiltonian depending only on particle configurations. In the end this should be a starting point for a non-equilibrium statistical mechanics theory.

References

[1] M.P. Ariza and M. Ortiz *Discrete crystal elasticity and discrete dislocations in crystals.* Arch. Rational Mech. Anal., **178** (2005), 149–226.

[2] P. Cermelli *Material symmetry and singularities in solids.* R. Soc. Lond. Proc. Ser. A Math. Phys. Eng. Sci., **455** (1999), 299–322.

[3] K. Kondo. *On the analytical and physical foundations of the theory of dislocations and yielding by the differential geometry of continua.* Int. J. Engng. Sci., **2** (1964),219–251.

[4] E. Kröner. *Allgemeine Kontinuumstheorie der Versetzungen und Eigenspannungen.* Arch. Rational Mech. Anal., **4** (1960), 273–334.

[5] S. Luckhaus, and L. Mugnai *On a mesoscopic many-body Hamiltonian describing elastic shears and dislocations.* Submitted paper (2009).

Thermodynamics and evolutionary genetics

Ingo Müller

Thermodynamics and evolutionary genetics have something in common. Thus the randomness of mutation of cells may be likened to the random thermal fluctuations in a gas. And the probabilistic nature of entropy in statistical thermodynamics can be carried over to a population of haploid and diploid cells without any conceptual change. The energetic potential wells, in which the atoms of a liquid are caught, correspond in genetics – to selective advantages for some phenotype over others. Thus the eventual stable state in a population comes about as a compromise in the universal competition between entropy and energy.

A population is discussed in which energetically equivalent alleles A and a are present. They undergo mutations of the type $A \leftrightarrow a$ and their entropy may be calculated as an entropy of mixing, so that without selection natural selection

or selection by a breeder the tend to an equi-distribution. If there is selection, it may be that cells of type a have an evolutionary advantage, or it may be that both types, A or a have an evolutionary advantage, if they are rare. In the latter case there is the possibility of a phase transition. In both cases there is a competition between mutation and selection, which leads to a maximum of entropy under the constraint of the selective advantage. Equilibrium fluctuations in the distribution of cells provide a possibility of survival of the population under a change of environment.

References

[1] I. Müller, *Thermodynbamics and evolutionary genetics*, Cont. Mech. and Thermodyn. **21** (2010).

Twisting An Open Knotted Elastic Rod

Sébastien Neukirch
(joint work with Basile Audoly, Nicolas Clauvelin)

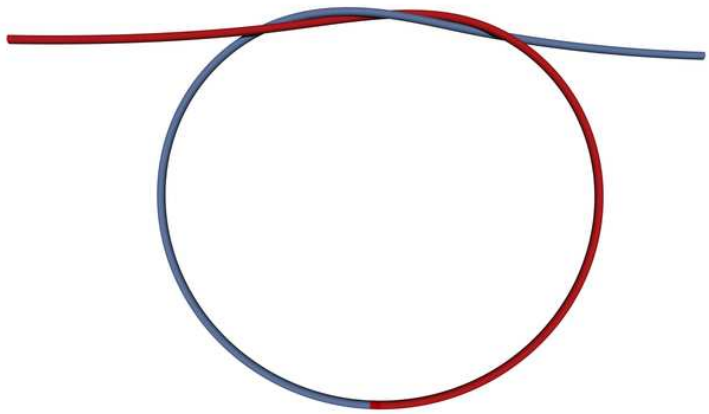

Figure 1. An open trefoil knot tied on an elastic filament. As the pulling tension is increased the loop radius decreases. Self-contact takes place in the braid region.

Knots are found in everyday life, shoe lacing being probably the most common example. They are also essential in a number of activities such as climbing and sailing. In science, knots have long been studied in the field of mathematics, the main motivation being to propose a topological classification of the various knot types, see e.g. the review by [1]. Recently, there has been an upsurge of interest in knots in the biological context: knots form spontaneously in many long polymers

chains such as DNA [2] or proteins, and have been tied on biological filaments [3]. Knotted filaments have a lower resistance to tension than unknotted ones and break preferably at the knot [5, 4]. Despite a wide range of potential applications, the mechanics of knots is little advanced. The present paper is an attempt to approach knots from a mechanical perspective by using a well-established model of thin elastic rods. To go beyond a purely geometrical description of knots, it is natural to formulate the problem in the framework of the theory of elasticity.

In the present work, we study the limit of *loose* knots, when the total contour length captured in the knot is much larger than the radius of the filament. In this limit, it is possible to use a Cosserat type model and describe the rod as an inextensible curve embedded with a material frame, obeying Kirchhoff equations; as we show, the equilibria of open knots can be solved analytically in this limit. Self-contact in continuum mechanics, and in the theory of elastic rods in particular, leads to problems that are both interesting and difficult. This comes from the fact that the set of points in contact is not known in advance — in fact, not even the topology of this set is known. This paper builds up on prior work by [6], who characterizes the smoothness of the contact force in equilibria of elastic rods, and by [7], who write down the Kirchhoff equations for rods in self-contact explicitly, including the unknown contact force. These equations have been solved by numerical continuation in specific geometries by [7, 8, 9]. In these papers, the authors simultaneously solve for the nonlinear Kirchhoff equations and for the unknown contact forces, but not for the contact topology which is postulated.

The mechanical problem considered here is the following. We solve the Kirchhoff equations for an infinite rod, with clamped boundary conditions at both endpoints at infinity. The rod is inextensible, unshearable and its weight is neglected; bending and twisting moments are related to curvature and twist by a linear constitutive law but geometric non-linearities are retained. Topology of the centerline is a prescribed knot shape (we consider trefoil and cinquefoil knots). This knotted shape is enforced by self-contact forces, which are taken into account in the equations of equilibrium. The rod is loaded under combined tension force T and twisting moment U at its endpoints; this loading is captured by a single dimensionless parameter, $\overline{U}$. We derive a family of solutions of the boundary-value problem depending on the loading parameter $\overline{U}$, which is asymptotically valid for small ϵ.

References

[1] M. Tabor, and I. Klapper *The dynamics of knots and curves (part I)*, Nonlinear science today **4** (1994), 7–13.

[2] V. Katritch, and J. Bednar, and D. Michoud, and R.G. Scharein, and J. Dubochet, and A. Stasiak *Geometry and physics of knots*, Nature **384** (1996), 142–145.

[3] Y. Arai, and R. Yasuda, and K. Akashi, and Y. Harada, and H. Miyata, and K. Kinosita, and H. Itoh *Tying a molecular knot with optical tweezers*, Nature **399** (1999), 446–448.

[4] P. Pieranski, and S. Kasas, and G. Dietler, and J. Dubochet, and A. Stasiak *Localization of breakage points in knotted strings*, New Journal of Physics **3** (2001), 10.1–10.13.

[5] A.M. Saitta, and P.D. Soper, and E. Wasserman, and M.L. Klein *Influence of a knot on the strength of a polymer strand*, Nature **399** (1999), 46–48.

[6] F. Schuricht, and H. von der Mosel, *Euler-Lagrange Equations for Nonlinearly Elastic Rods with Self-Contact* Archive for Rational Mechanics and Analysis **168** (2003), 35–82.
[7] B. Coleman, and D. Swigon, *Theory of Supercoiled Elastic Rings with Self-Contact and Its Application to DNA Plasmids* Journal of Elasticity **60** (2000), 173–221.
[8] G.H.M. van der Heijden, and S. Neukirch, and V.G.A. Goss, and J.M.T. Thompson, *Instability and self-contact phenomena in the writhing of clamped rods* International Journal of Mechanical Sciences **45** (2003), 161–196.
[9] S. Neukirch, *Extracting DNA Twist Rigidity from Experimental Supercoiling Data* Physical Review Letters **93** (2004), 198107-1–198107-4.

Stripe Patterns and the Eikonal Equation

Mark A. Peletier
(joint work with Marco Veneroni)

1. Introduction

In this note we describe the behaviour of a stripe-forming system that arises in the modelling of block copolymers. Part of the analysis concerns a new formulation of the eikonal equation in terms of *projections*. For precise statements of the results, complete proofs, and references, we refer to [5] and [4].

1.1. **Diblock Copolymers.** In [5] we study the formation of stripe-like patterns in a specific two-dimensional system that arises in the modelling of AB diblock copolymers. This system is defined by an energy $\mathcal{G}_\varepsilon$ that admits locally minimizing stripe patterns of width $O(\varepsilon)$, and the aim is to study the properties of the system as $\varepsilon \to 0$. Below we will show that any sequence u_ε of patterns for which $\mathcal{G}_\varepsilon(u_\varepsilon)$ is bounded becomes stripe-like; in addition, the stripes become increasingly straight and uniform in width.

The energy functional is

$$\mathscr{F}_\varepsilon(u) = \begin{cases} \varepsilon \displaystyle\int_\Omega |\nabla u| + \frac{1}{\varepsilon} d(u, 1-u), & \text{if } u \in K, \\ \infty & \text{otherwise.} \end{cases} \tag{1}$$

Here Ω is an open, connected, and bounded subset of $\mathbb{R}^2$ with C^2 boundary, d is the Monge-Kantorovich distance, and

$$K := \left\{ u \in BV(\Omega; \{0,1\}) \,:\, \fint_\Omega u(x)\,dx = \frac{1}{2} \text{ and } u = 0 \text{ on } \partial\Omega \right\}.$$

We introduce a rescaled functional $\mathcal{G}_\varepsilon$ defined by

$$\mathcal{G}_\varepsilon(u) := \frac{1}{\varepsilon^2}\Big(\mathscr{F}_\varepsilon(u) - |\Omega|\Big).$$

The interpretation of the function u and the functional $\mathscr{F}_\varepsilon$ are as follows.

The function u is a characteristic function, whose support corresponds to the region of space occupied by the A part of the diblock copolymer; the complement (the support of $1-u$) corresponds to the B part. The boundary condition $u = 0$ in

K reflects a repelling force between the boundary of the experimental vessel and the A phase.

The functional $\mathscr{F}_\varepsilon$ contains two terms. The first term penalizes the interface between the A and the B parts, and arises from the repelling force between the two parts; this term favours large-scale separation. In the second term the the Monge-Kantorovich distance d appears; this term is a measure of the spatial separation of the two sets $\{u = 0\}$ and $\{u = 1\}$, and favours rapid oscillation. The combination of the two leads to a preferred length scale, which is of order ε in the scaling of (1).

1.2. **A non-oriented version of Eikonal equation.** At finite $\varepsilon > 0$, structures with small $\mathcal{G}_\varepsilon$ resemble parallel stripes of thickness roughly 2ε. As $\varepsilon \to 0$, these stripes become dense, and the limiting structure can be interpreted as a field of infinitesimal stripes—a field of orientations.

A natural mathematical object for the representation of such orientation fields, or line fields, is a *projection*. We define a projection to be a matrix P that can be written in terms of a unit vector m as $P = m \otimes m$. Such a projection matrix has a range and a kernel that are both one-dimensional, and if necessary one can identify a projection P with its range, i.e. with the one-dimensional subspace of $\mathbb{R}^2$ onto which it projects. Note that the independence of the sign of m—the unsigned nature of a projection—can be directly recognized in the formula $P = m \otimes m$.

We define $\operatorname{div} P$ as the vector-valued function whose i-th component is given by $(\operatorname{div} P)_i := \sum_{j=1}^{2} \partial_{x_j} P_{ij}$. We consider the following problem. Let Ω be an open subset of $\mathbb{R}^2$. Find $P \in L^\infty(\Omega; \mathbb{R}^{2\times 2})$ such that

$$
\begin{aligned}
&\text{(2a)} && P^2 = P && \text{a.e. in } \Omega,\\
&\text{(2b)} && \operatorname{rank}(P) = 1 && \text{a.e. in } \Omega,\\
&\text{(2c)} && P \text{ is symmetric} && \text{a.e. in } \Omega,\\
&\text{(2d)} && \operatorname{div} P \in L^2(\mathbb{R}^2; \mathbb{R}^2) && \text{(extended to 0 outside } \Omega),\\
&\text{(2e)} && P \operatorname{div} P = 0 && \text{a.e. in } \Omega.
\end{aligned}
$$

The first three equations encode the property that $P(x)$ is a projection, in the sense above, at almost every x. The sense of property (2d) is that the divergence of P (extended to 0 outside Ω), in the sense of distributions in $\mathbb{R}^2$, is an $L^2(\mathbb{R}^2)$ function, which, in particular, implies

$$Pn = 0 \quad \text{in the sense of traces on } \partial\Omega.$$

The exponent 2 in (2d) is critical in the following sense. Obvious possibilities for singularities in a line field are jump discontinuities ('grain boundaries') and target patterns (see Figure 1).

At a grain boundary the jump in P causes $\operatorname{div} P$ to have a line singularity, comparable to the one-dimensional Hausdorff measure; condition (2d) clearly excludes that possibility. For a target pattern the curvature κ of the stripes scales as $1/r$, where r is the distance to the center; then $\int \kappa^p$ is locally finite for $p < 2$, and diverges logarithmically for $p = 2$. The cases $p < 2$ and $p \geq 2$ therefore distinguish between whether target patterns are admissible ($p < 2$) or not.

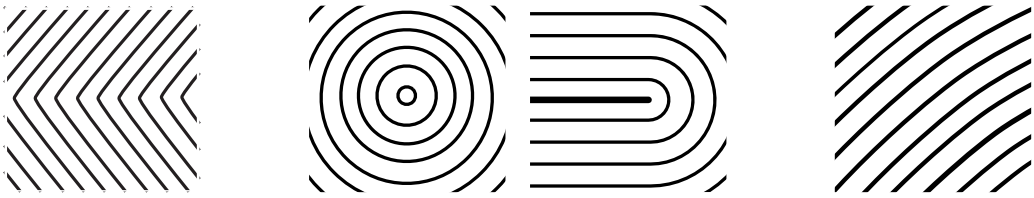

FIGURE 1. Canonical types of stripe variation in two dimensions: grain boundary (left), target and U-turn patterns (middle) and smooth directional variation (right). The left and middle types are excluded by (2d).

Given the regularity provided by (2d), the final condition (2e) represents the condition of parallelism, as a calculation for a smooth unit-length vector field $m(x)$ shows:

(3)

$$0 = P \operatorname{div} P = m(m \cdot (m \operatorname{div} m + \nabla m \cdot m)) = m \operatorname{div} m + m(m \cdot \nabla m \cdot m) = m \operatorname{div} m,$$

where the final equality follows from differentiating the identity $|m|^2 = 1$. For this smooth case the orientation field P can also be interpreted as a solution of the eikonal equation $|\nabla u| = 1$, as follows. The solution vector field m is divergence-free by (3), implying that its rotation over 90 degrees is a gradient ∇u; from $|m| = 1$ it follows that $|\nabla u| = 1$. This little calculation also shows that the interpretation of m in $P = m \otimes m$ is that of the stripe direction; P projects along the normal onto the tangent to a stripe.

1.3. **Main result.** The precise relation between the solutions of the non-oriented eikonal equation and the block copolymer energy functionals is the following:

Theorem 1. *The rescaled functional $\mathcal{G}_\varepsilon$ Gamma-converges to the functional*

$$\mathcal{G}_0(P) := \begin{cases} \dfrac{1}{8} \displaystyle\int_\Omega |\operatorname{div} P(x)|^2 dx & \text{if } P \in \mathcal{K}_0(\Omega) \\ +\infty & \text{otherwise} \end{cases}$$

Here the admissible set $\mathcal{K}_0(\Omega)$ is the set of solutions of (2). The topology of the Gamma-convergence in this case is the strong topology of measure-function pairs in the sense of Hutchinson [2]. The main tool in the proof of Theorem 1 is an explicit lower bound on the energy $\mathcal{G}_\varepsilon$ originally derived in [3]. This inequality gives a tight connection between low energy on one hand and specific properties of the geometry of the stripes on the other.

We refer to [4, 5] for the details and an extended discussion.

REFERENCES

[1] M. Muster, *Computing certain invariants of topological spaces of dimension three*, Topology **32** (1990), 100–120.

[2] J. E. Hutchinson. *Second fundamental form for varifolds and the existence of surfaces minimising curvature*, Indiana Univ. Math. J., **35** (1986), 45–71.

[3] M. A. Peletier and M. Röger. *Partial localization, lipid bilayers, and the Elastica functional*, Archive for Rational Mechanics and Analysis, **193** (2009), 475–537.
[4] M. A. Peletier and M. Veneroni. *Non-oriented solutions of the eikonal equation*. Arxiv preprint arXiv:0811.3928 (2008). Submitted.
[5] M. A. Peletier and M. Veneroni. *Stripe patterns in a model for block copolymers*. Arxiv preprint arXiv:0902.2611 (2009), *Accepted for publication in* Mathematical Models and Methods in Applied Sciences.

Criticality in material behaviour

Francisco J. Pérez-Reche
(joint work with Lev Truskinovsky and Giovanni Zanzotto)

Scale-free behaviour, also referred to as criticality, has been observed in many natural systems and processes such as earthquakes, epidemic outbreaks or solar flares [1]. In particular, criticality is ubiquitous within materials science. For instance, it has been observed in the intermittent response of metals being deformed plastically [2] or the acoustic events (avalanches) detected during the martensitic transformation [3, 4, 5]. The most frequently given experimental evidence for criticality is the power-law probability density function, $p(A) \propto A^{-\alpha}$, obeyed by the observed quantities, A, such as the magnitude of earthquakes or the size of acoustic emission signals detected during the martensitic transformation. It is easy to prove that power-law is the only functional dependence remaining invariant under changes in scale of the observable A.

Critical phenomena in natural systems has been widely studied in connection to second-order phase transitions such as, for instance, the paramagnetic $\rightarrow$ ferromagnetic transition undergone by magnets when cooled below a certain critical temperature, T_c, the so-called Curie temperature [6]. At T_c, the fluctuations of the order parameter (magnetisation) are infinitely large and there is no characteristic scale in the system. The Renormalization Group is a systematic and powerful framework allowing the criticality in second-order phase transitions to be described [7, 8]. Roughly speaking, the renormalization group consists in analysing the effect of changing the scale (Renormalization Group transformation, RGT) of systems. Critical points responsible for second-order phase transitions are associated with critical fixed points under RGT which represent scale-free systems. The set of all systems flowing towards a certain critical fixed point under RGT share the same critical behaviour and define a universality class. This idea is one of the greatest achievements of the renormalization group as it allowed the concept of universality (i.e., different systems share the same critical behaviour) to be understood.

The ubiquity of criticality observed in externally driven systems cannot be explained in terms of the existence of critical fixed points only. Indeed, in addition to the existence of at least one critical fixed point, a mechanism self-organising the system towards the critical manifold of the critical fixed point is necessary.

This defines the concept of Self-Organised Criticality (SOC)[1]. For instance, in martensites, the distribution of size of the avalanches attain a power-law only after multiple cycling through the martensitic transformation [10, 5]. We have proposed that the interplay of reversible phase transformation with concurrent activity of defects such as dislocations, allows the system to attain the optimal amount of disorder and therefore become critical [11, 12].

In the present talk we have concentrated on the study of the critical behaviour displayed by the Random Snap-Spring Model (RSSM) with athermal dynamics (i.e., $T = 0$) which is usually a good approximation to the kinetics of non-diffusive structural transformations in solids [13]. In the limit of slow driving, the model exhibits two drastically different types of critical non-equilibrium steady states [14]. One of them is related to the existence of a critical point for a certain value of the disorder, r_o. This corresponds to classical criticality in the sense that it requires fine tuning of the disorder in a way analogous to the tuning of temperature necessary to reach criticality in magnets [15]. Self-organisation to criticality is absent in this regime and systems with generic disorder are therefore not expected to lie on a critical manifold in general. The other critical steady state observed in the model is a self-organised criticality which is insensitive to disorder. This regime is reminiscent of the criticality associated with the pinning-depinning (PD) transition where the disorder r is an irrelevant parameter [16], i.e., the PD critical manifold exist for a finite interval of r. Owing to the irrelevance of r, it has been established that systems displaying a PD transition with generic disorder display SOC towards one of the PD universality classes in the limit of infinitely slow driving [17, 18]. The crossover between the two types of criticality in the RSSM is determined by the mode of driving. As one moves from 'soft' to 'hard' driving the universality class of the critical point changes from OD (classical order-disorder [15]) to QEW (quenched Edwards-Wilkinson, one of the possible PD universality classes [19]).

References

[1] M. E. J. Newman, *Power laws, Pareto distributions and Zipf's law*, Contemporary Physics **46** (2004), 323 – 351.

[2] D. M. Dimiduk, C. Woodward, R. LeSar, and M. D. Uchic, *Scale-Free Intermittent Flow in Crystal Plasticity*, Science **312** (2006), 1188–1190.

[3] E. Vives, J. Ortín, L. Mañosa, I. Ràfols, R. Pérez-Magrané, and A. Planes, *Distribution of Avalanches in Martensitic Transformations*, Phys. Rev. Lett. **72** (1994), 1694–1697.

[4] F. J. Pérez-Reche, B. Tadić, L. Mañosa, A. Planes, and E. Vives, *Driving Rate Effects in Avalanche-Mediated First-Order Phase Transitions*. Phys. Rev. Lett. **93** (2004), 195701.

[5] E. Vives, D. Soto-Parra, L. Mañosa, R. Romero, and A. Planes, *Driving-induced crossover in the avalanche criticality of martensitic transitions*, Phys. Rev. B **80** (2009), 180101(R).

[6] H. E. Stanley, *Introduction to Phase Transitions and Critical Phenomena*, Oxford University Press, New York, 1983.

[7] K. G. Wilson, *Renormalization Group and critical phenomena. I. Renormalization Group and the Kadanoff scaling picture*, Phys. Rev. B **4** (1971), 3174–3183.

[1]Note that the definition of SOC given here is slightly different to the original definition given in Ref. [9] which does not establish an explicit link with critical fixed points under RGT.

[8] M. E. Fisher, *Renormalization group theory: Its basis and formulation in statistical physics*, Rev. Mod. Phys. **70** (1998), 653–681.
[9] P. Bak, C. Tang, and K. Wiesenfeld, *Self-Organized Criticality: An Explanation of* $1/f$ *Noise*, Phys. Rev. Lett. **59** (1987), 381 – 384.
[10] F. J. Pérez-Reche, M. Stipcich, E. Vives, L. Mañosa, and A. Planes, *Kinetics of martensitic transitions in Cu-Al-Mn under thermal cycling: Analysis at multiple length scales*, Phys. Rev. B **69** (2004), 064101.
[11] F. J. Pérez-Reche, L. Truskinovsky, and G. Zanzotto, *Training-induced criticality in martensites*, Phys. Rev. Lett. **99** (2007), 075501.
[12] F. J. Pérez-Reche, L. Truskinovsky, and G. Zanzotto, *Martensitic transformations: from continuum mechanics to spin models and automata*, Continuum Mech. Thermodyn. **21** (2009), 17–26.
[13] F. J. Pérez-Reche, E. Vives, L. Mañosa, and A. Planes, *Athermal character of structural phase transitions*, Phys. Rev. Lett. **87** (2001), 195701.
[14] F. J. Pérez-Reche, L. Truskinovsky, and G. Zanzotto, *Driving-Induced Crossover: From Classical Criticality to Self-Organized Criticality*, Phys. Rev. Lett. **101** (2008), 230601.
[15] J. P. Sethna, K. A. Dahmen, and C. R. Myers, *Crackling noise*, Nature **410** (2001), 242–250.
[16] O. Narayan and D. S. Fisher, *Threshold critical dynamics of driven interfaces in random media*, Phys. Rev. B **48** (1993), 7030–7042.
[17] R. Dickman, M. A. Muñoz, A. Vespignani, and S. Zapperi, *Paths to Self-Organized Criticality*, Braz. J. Phys. **30** (2000), 27–41.
[18] M. Alava, *Scaling in self-organized criticality from interface depinning?*, J. Phys.: Condens. Matter **14** (2002), 2353–2360.
[19] A. L. Barabási and H. E. Stanley, *Fractal Concepts in Surface Growth*, Cambridge University Press, Cambridge (UK), 1995.

Criticality in martensite

Oguz Umut Salman

Self Organized Criticality (SOC) is a concept introduced in the early 90's to unify the understanding of natural systems governed by different physical laws. The main motivation of self organization theories is to find an explanation to the fact that many natural systems exhibit structural and dynamical complexity even though the laws of physics that govern interactions between the elements of those systems are often simple. In other words, self-organization seeks to discover the general rules under which complexity may occur, the forms which it can take and methods of predicting the changes to the structure that will result from changes to the underlying system [1].

Even though there is no exact definition for complexity, an important signature of complexity is *scale-invariance*. The analysis of complex shapes and time-series signals has led to the discovery that when they are viewed at different levels of magnification, their structures often appear to look roughly the same, hence they are *scale-invariant* or *self-similar*. This property was termed as *fractals* by Mandelbrot [4] but the origin was not understood. Mathematically scale-invariance can be captured by a power law, which will be crucial in the following discussions, and it is given by

$$P(A) = A^{-\beta}, \tag{1}$$

where $P(A)$ is the probability density of some characteristic quantity A and β called as *scaling exponent*. This power law relation has the property of scale-invariance. More precisely, decreasing the scale corresponds to see finer details of the spectrum having the same qualitative relationship with higher values, i.e., the scaling leaves the basic form of the spectrum of A unchanged. Note that only power laws have this unique feature.

In this talk, we have focussed on the study of the critical (scale-free) behavior of martensitic phase transformations. The kinetic of martensitic phase transformations has been studied in several experimental works and it has been shown that acoustic emission (AE) generated during a martensitic transformation follows a power law behavior for both amplitude (A) and durations (T) of the signal [3]. However, the origin of avalanches and of the scale-free character of behavior in 3D real martensites are not fully understood. Here, we study this problem using classical mechanics that takes all of the principal features of martensites into account, i.e., the three dimensional nature of transformation, inertial effects, long-range interactions corresponding to a real crystallography (cubic-to-tetragonal) and real experimental parameters (elastic constants, interfacial energy, dissipation and mass density) of FePd alloy.

In three dimensions, a cubic-to-tetragonal transition can be described by two deviatoric strains e_2 and e_3 representing shear deformations on $\{110\}$-type planes in the $< \bar{1}10 >$-type directions and they are defined as

$$e_2 = \frac{1}{\sqrt{2}}(\epsilon_{xx} - \epsilon_{yy}), e_3 = \frac{1}{\sqrt{6}}(\epsilon_{xx} + \epsilon_{yy} - 2\epsilon_{zz}). \tag{2}$$

The remaining components of the symmetry-adapted strain tensor are

$$e_1 = \frac{1}{\sqrt{3}}(\epsilon_{xx} + \epsilon_{yy} + \epsilon_{zz}), e_4 = \epsilon_{xy} + \epsilon_{yx}, e_5 = \epsilon_{xz} + \epsilon_{zx}, e_6 = \epsilon_{yz} + \epsilon_{zy}, \tag{3}$$

where $\epsilon_{ij} = \frac{1}{2}(\frac{\partial u_i}{\partial x_j} + \frac{\partial u_j}{\partial x_i})$ and u_i is the displacement vector.

A cubic-to-tetragonal transition can be described by the functional given by

$$F_{tetra} = A_2(e_2^2 + e_3^2) + A_4 e_3(e_3^2 - 3e_2^2) + A_6(e_2^2 + e_3^2)^2. \tag{4}$$

The form of this functional guarantees that there are four degenerate energy minima corresponding to three tetragonal variants and the austenite phase at the transition temperature. The coefficient A_2 can be tuned to change the depth of wells in order to incorporate the temperature dependance. The other coefficients can be tuned using experimental data. The harmonic strain energy contribution due to shear strains is given by

$$F_{shear} = A_3(e_4^2 + e_5^2 + e_6^2). \tag{5}$$

The volume change associated with the transformation is incorporated in the free energy by adding the term

$$F_{bulk} = A_1(e_1 - K(e_2^2 + e_3^2))^2. \tag{6}$$

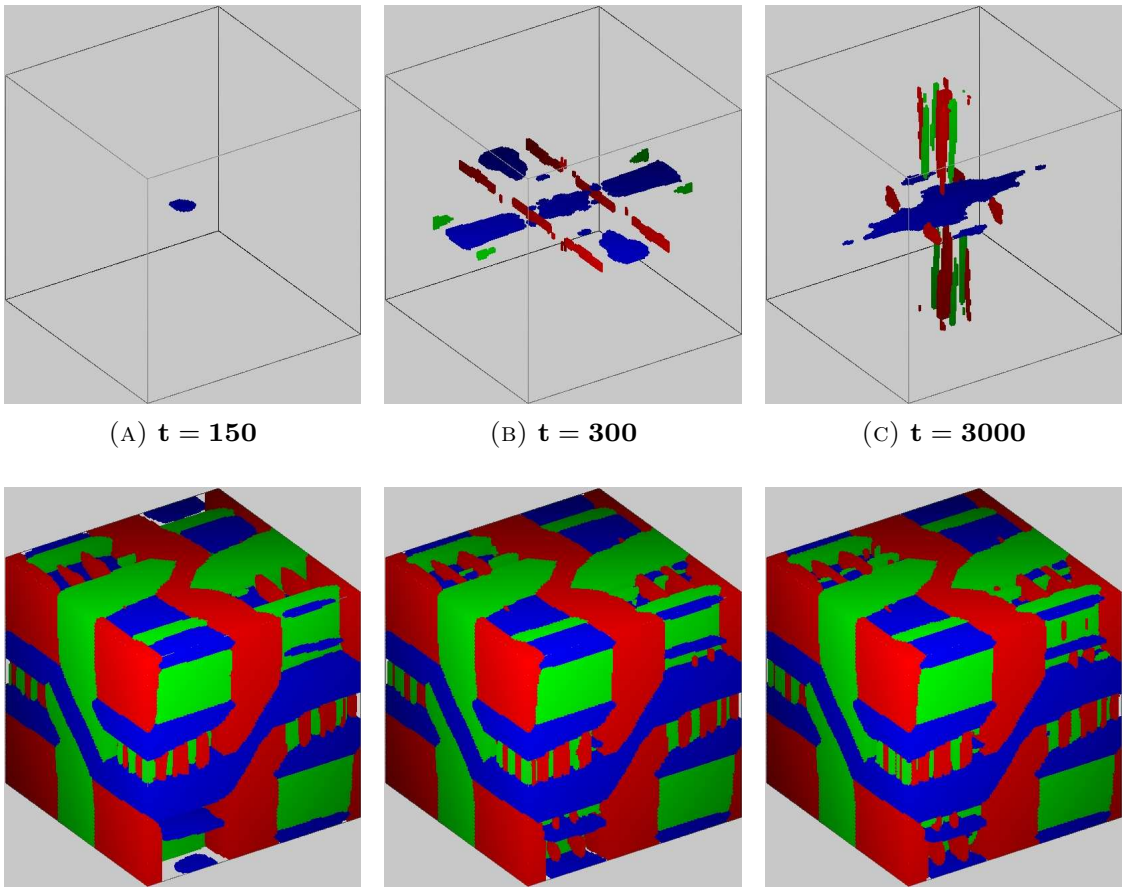

(A) **t = 150** (B) **t = 300** (C) **t = 3000**

(D) **t = 13000** (E) **t = 15000** (F) **t = 16000**

FIGURE 1. *Time evolution of the system.*

The Ginzburg energy that penalizes the interfaces is written only in terms of primary order parameters e_2 and e_3 in the spirit of Landau theory and is given by

$$F_G = \frac{\beta}{2}(|\nabla e_2|^2 + |\nabla e_3|^2). \tag{7}$$

Finally, the total free energy reads

$$\mathscr{F}_{GL} = \int_V \Big\{ F_L + F_G \Big\} d\mathbf{r}, \tag{8}$$

where $F_L = F_{tetra} + F_{shear} + F_{bulk}$. Finally, we add the kinetic energy by $\mathscr{T} = \int_V \rho \dot{u}_i^2$ and the dissipation by $\mathscr{R} = \int_V \gamma \dot{e}_i^2$ for $i = 1, 3$. Finally, the dynamical equation is given by $\frac{d}{dt}\frac{\delta \mathscr{L}}{\delta \dot{u}_i} - \frac{\delta \mathscr{L}}{\delta u_i} = -\frac{\delta \mathscr{R}}{\delta \dot{u}_i}$, where $\mathscr{L} = \int_V \big\{T - (F_L + F_G)\big\} d\mathbf{r}$.

To initiate the transition a single defect is put in the middle of the system. At $t = 0$, the displacement vector u_i vanishes at every point. Therefore, there is no quenched (pre-existent) disorder in the system.

Figure 1 displays the evolution of the microstructure from the nucleation of variants of martensite starting around the perturbation in the middle of the system until the final state reached under constant cooling rate. It is clear from figs. 1(a)-1(c) that the austenite transforms first into a single variant of martensite

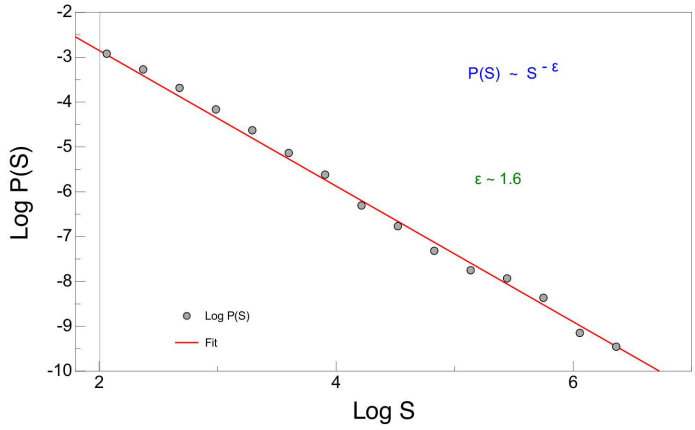

(A)

FIGURE 2. *Log-log plot of distribution of avalanche surfaces P(S) with scaling exponent* $\epsilon = 1.6$.

(variant 3 shown with blue color) around the defect and then other variants appear (variant 1 and 2 shown with green and red colors, respectively and the austenite is transparent) in an auto-catalytic way. Finally, as seen from fig. 1(d)-1(f), the austenite is completely transformed into the variants of martensite. Note that each pair of variants in a cubic-to-tetragonal transition are twin related and all the twins are compound twins having $\{110\}_{cubic}$ planes as obtained in the simulations.

Indeed, the energy dissipation occurs when either austenite transforms into one variant of martensite or one of already existing variants of martensite transforms into one of the other variants. The statistical analysis of the dissipated energy during the transformation for distributions of the avalanche characteristics: (durations T, amplitudes A and surfaces S) lead to the power-laws: $P(A) \sim A^{-\alpha}$, $P(T) \sim T^{-\tau}$, and $P(S) \sim S^{-\epsilon}$ with exponents $\alpha = 2.15$, $\tau = 2.4$ and $\epsilon = 1.6$ (see fig. 2). These results are also in good agreement with experimental observations [2].

This result shows that the critical state can be reached in the presence of inertial effects in three dimensions without any external disorder (static or dynamic) which has been claimed to be the reason of critical behavior in martensites [6, 8, 5, 7]. The inertial effects provide the system a way of passing through more metastable states resulting in scale-free behavior that clearly lacks in the purely dissipative approaches.

REFERENCES

[1] P. Bak, *How nature works*, Springer-Verlag (1996).
[2] E. Bonnot, L. Manosa, A. Planes, D. Soto-Parra, E. Vives, B. Ludwig, C. Strothkaemper, T. Fukuda, and T. Kakeshita, *Acoustic emission study of the FCC-FCT martensitic transition in FePd*, Unpublished (2008).
[3] E. Vives, J. Ortín, L. Mañosa, I. Ràfols, R. Pérez-Magrané, and A. Planes, *Distributions of avalanches in martensitic transformations*, Phys. Rev. Lett., **72** (1994), 1694–1697.
[4] M. Buchanan, *Ubiquity*, Weidenfeld and Nicholson (2000).

[5] K. Dahmen, and J.P. Sethna, *Hysteresis, avalanches, and disorder-induced critical scaling: A renormalization-group approach*, Phys. Rev. B., **53** (1996), 14872–14905.
[6] J.P. Sethna, K. Dahmen, S. Kartha, J.A. Krumhansl, B.W. Roberts, and J.D. Shore, *Hysteresis and hierarchies: Dynamics of disorder-driven first-order phase transformations*, Phys. Rev. Lett, **70** (1993), 3347–3350.
[7] F.J. Pérez-Reche, L Truskinovsky, and G Zanzotto, *Training-Induced Criticality in Martensites*, Phys. Rev. Lett., **99** (2007), 0755011–0755014.
[8] O. Perković, K. Dahmen, and J.P. Sethna, *Avalanches, Barkhausen Noise, and Plain Old Criticality*, Phys. Rev. Lett., **75** (1995), 4528–4531.

From Atomistic Models to Linear Elasticity

Bernd Schmidt

The relation of atomistic and continuum models of matter is an important and very active area of current research, both from a computational and from the analytical point of view. Ultimately, the elastic moduli of solids should be derivable from atomistic models. The main aim of this note is to report on recent results on rigorous derivations of effective linearized theories for elastic bodies starting from atomistic models, see [7]. Our approach thus combines the derivation of linearized theories from nonlinear models (see [3] for a rigorous approach in the pure continuum setting) with the passage from atomistic to continuum theory (see, e.g., in [5] for thin films and the results [4, 2] on the Cauchy-Born rule).

More precisely, we will derive linear elasticity theory from atomistic models by means Γ-convergence. In particular, we will obtain the simultaneous limit when both the number of atoms tends to infinity (i.e., when the interatomic distances tend to zero) and the strains within the material become infinitesimally small. Our approach generalizes a recent result of Braides, Solci and Vitali [1]. In particular, we study mass spring models with full nearest neighbor (NN) and next-to-nearest neighbor (NNN) pair interactions. We also consider boundary value problems where a part of the boundary is free.

Consider the atomistic reference configuration $\varepsilon\mathcal{L} \cap \Omega$, where $\Omega \subset \mathbb{R}^d$ (the 'macroscopic region' occupied by the material) is a Lipschitz domain, $\mathcal{L} = A\mathbb{Z}^d$, $A \in \mathbb{R}^{d\times d}$ with $\det A > 0$, a Bravais lattice (the 'atomic crystal') and $\varepsilon \ll 1$ is a small parameter (the 'interatomic distance'). Atomic deformations are mappings

$$y : \varepsilon\mathcal{L} \cap \Omega \to \mathbb{R}^d.$$

In order to efficiently describe these deformation, we will need some book keeping: Choose a numbering $z^1, \dots, z^{2^d}$ of $A\{-\frac{1}{2}, \frac{1}{2}\}^d$ and let

$$Z = (z^1, \dots, z^{2^d}) \in \mathbb{R}^{d\times 2^d}$$

(cf. Fig. 1). Let $x' \in \varepsilon\mathcal{L}'$ denote the centers of the unit cells $\varepsilon A(z+[0,1)^d)$, $z \in \mathbb{Z}^d$. Now the main object that encodes all the relative displacements of atoms in one cell is the following *discrete gradient*:

$$\bar{\nabla} y(x') := \varepsilon^{-1}\Big(y(x'+\varepsilon z^1) - y(x'), \dots, y(x'+\varepsilon z^{2^d}) - y(x')\Big) \in \mathbb{R}^{d\times 2^d},$$

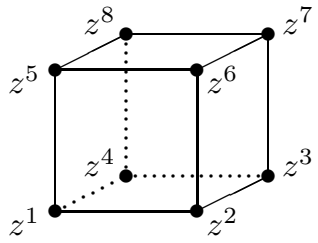

FIGURE 1. Reference unit cell.

where we have interpolated on $\varepsilon\mathcal{L}'$ by setting $y(x') := \frac{1}{2^d}\sum_{i=1}^{2^d} y(x'+\varepsilon z^i)$. E.g., the discrete gradient of $x \mapsto Gx$, $G \in \mathbb{R}^{d\times d}$, is GZ.

Our main structural assumption is that the energy of a deformation $y : \varepsilon\mathcal{L}\cap\Omega \to \mathbb{R}^d$ be given as a sum of individual *cell energies* as follows.

$$E_\varepsilon(y) = \sum_{x'} W_\varepsilon(x', \bar{\nabla} y(x')), \quad W_\varepsilon(x', \cdot) = W_{\text{cell}}(\cdot) + W_{\text{surface}}(x', \cdot).$$

For simplicity, we will neglect W_{surface} in the sequel and refer to [7] for further details on surface terms. Typical examples of admissible energy functionals are given by suitable *mass spring models* (cf Fig. 2).

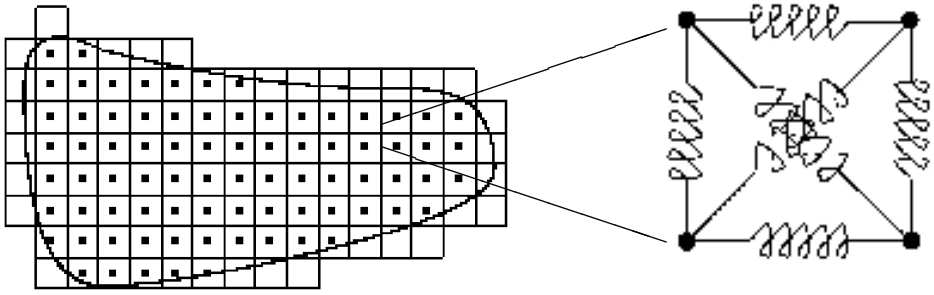

FIGURE 2. A 2d NN & NNN mass spring model.

Basic Assumption.

(1) Frame indifference: $\forall\, R \in SO(d), c \in \mathbb{R}^d, F \in \mathbb{R}^{d\times 2^d}$:

$$W_{\text{cell}}(RF + (c, \dots, c)) = W_{\text{cell}}(F).$$

(2) $W_{\text{cell}} \geq 0$ and $W_{\text{cell}}(F) = 0$ iff

$$\exists R \in SO(d), c \in \mathbb{R}^d \text{ s.t. } F_i = Rz^i + c.$$

(3) W_{cell} is C^2 near $\bar{SO}(d) = \{RZ : R \in SO(d)\}$. The Hessian $Q_{\text{cell}} = D^2 W_{\text{cell}}(Z)$ is positive definite on the orthogonal complement of the subspace spanned by infinitesimal translations $(c, \dots, c)$ and rotations FZ, $F^T = -F$.

(4) W_{cell} grows at infinity at least quadratically on the orthogonal complement of the subspace spanned by infinitesimal translations.

Suppose $\partial\Omega_* \subset \partial\Omega$ (the 'Dirichlet boundary') has positive $\mathcal{H}^{d-1}$-measure and consider the space

$$\mathcal{A}_\varepsilon(g, \partial\Omega_*, \Omega) = \{u : \varepsilon\mathcal{L} \cap \Omega \to \mathbb{R}^d : u = g \text{ on Dirichlet boundary cells}\}$$

of admissible lattice displacements. (See [7] for the precise definition of *Dirichlet boundary cells*, where Dirichlet boundary data are prescribed, and of the continuum analogue $H^1(g, \partial\Omega_*, \Omega)$ of $\mathcal{A}_\varepsilon(g, \partial\Omega_*, \Omega)$.) In order to derive linear elasticity from atomistic models, we prove a Γ-convergence result for the functionals

$$I_k(u) = \delta_k^{-2}\varepsilon_k^d E_\varepsilon(\mathrm{Id} + \delta_k u) = \delta_k^{-2}\varepsilon_k^d \sum_{x'} W_{\mathrm{cell}}(Z + \delta_k \bar{\nabla} u(x')),$$

when $\varepsilon_k, \delta_k \to 0$. Here a sequence of *discrete displacements* (u_k) is understood to converge to the *continuum displacement* $u : \Omega \to \mathbb{R}^d$ if suitable interpolations of u_k converge to u in L^2.

Additional assumption. If W_{cell} and W_{surface} are 'incompatible' or if $\partial\Omega_* \neq \partial\Omega$, then assume $\lim_k \delta_k^{-2}\varepsilon_k = 0$.

Theorem 1 (Compactness). If $I_k(u_k) \leq C$, then for a subsequence and after modification on non-Dirichlet boundary cells and suitable interpolation

(1) $u_k \rightharpoonup u$ for some $u \in H^1(g, \partial\Omega_*, \Omega)$.
(2) For (p. c. interpolations of) $\bar{\nabla} u_k$: $\bar{\nabla} u_k \rightharpoonup \nabla u \cdot Z$ in L^2.

Theorem 2 (Gamma-convergence). The functionals I_k Γ-converge to

$$I : H^1(g, \partial\Omega_*, \Omega) \to \mathbb{R}, \quad I(u) = \frac{1}{2 \det A} \int_\Omega Q_{\mathrm{cell}}(e(u) \cdot Z),$$

$e(u) = \frac{1}{2}((\nabla u)^T + \nabla u)$.

Theorem 3. If $I_k(w_k) - \inf I_k \to 0$, then (after modification on non-Dirichlet boundary cells)

$$\bar{\nabla} u_k \to \nabla u \cdot Z \text{ strongly in } L^2, \quad u \text{ the unique minimizer of } I.$$

Remarks.

(1) Manifestation of the Cauchy-Born rule: I is precisely the energy functional one would obtain by first passing from atomistic models to nonlinear elasticity by applying the Cauchy-Born rule and then passing from nonlinear to linear elasticity (cf. [3]).
(2) The condition $\varepsilon \ll \delta^2$ guarantees that surface contributions cannot dominate the bulk energy terms near the free boundary.
(3) Strong L^2-convergence of the gradients of minimizers (see Thm. 3) is new even for the nonlinear-to-linear continuum limit of [3], cf. [6].

References

[1] A. Braides, M. Solci and E. Vitali, *A derivation of linear elastic energies from pair-interaction atomistic systems*, Netw. Heterog. Media **2** (2007), 551–567.
[2] S. Conti, G. Dolzmann, B. Kirchheim and S. Müller, *Sufficient conditions for the validity of the Cauchy-Born rule close to $SO(n)$*, J. Eur. Math. Soc. (JEMS) **8** (2006), 515–539.
[3] G. Dal Maso, M. Negri and D. Percivale, *Linearized elasticity as Γ-limit of finite elasticity*, Set-valued Anal., **10** (2002), 165–183.

[4] G. Friesecke, F. Theil, *Validity and failure of the Cauchy-Born hypothesis in a two-dimensional mass-spring lattice*, J. Nonlinear Sci., **12** (2002), 445–478.
[5] B. Schmidt, *A derivation of continuum nonlinear plate theory from atomistic models*, SIAM Mult. Model. Simul. **5** (2006), 664–694.
[6] B. Schmidt, *Linear Gamma-limits of multiwell energies in nonlinear elasticity theory*, Contin. Mech. Thermodyn. **20** (2008), 375–396.
[7] B. Schmidt, *On the derivation of linear elasticity from atomistic models*, Netw. Heterog. Media **4** (2009), 789–812.

3d-Crystallization: FCC and HCP

Florian Theil
(joint work with Lisa Harris)

We study the asymptotic behavior of minimizers of classical pair energy systems in the limit where the number of particles tends to infinity. To be specific, we assume that the pair interaction energy between two point particles with positions $y, y' \in \mathbb{R}^3$ is given by $V(|y - y'|)$ for some potential $V : (0, \infty) \to \mathbb{R}$. The scaled pair-energy of an n-particle configuration $y \in \mathbb{R}^{3\times n}$ is then given by

$$E_n(\{y\}) = \frac{1}{n} \sum_{1\le i<j\le n} V(|y_i - y_j|).$$

It is known from numerical simulations that for sufficiently large n and $V(r) = r^{-12} - r^{-6}$ (the Lennard-Jones potential) the minimizers form slightly deformed subsets of a hexagonally close packed lattice (hcp). The hcp-lattice is one of the two lattices that solve the kissing problem, i.e. the number of nearest neighbors is 12. The other lattice with the same property is the fcc-lattice (face-centered-cubic). We can prove that for sufficiently strongly localized potentials V the minium of E_n is the energy per particle of a hcp or fcc lattice, depending on finer properties of V.

Definition Let $\mathcal{L} \subset \mathbb{R}^3$ be either a fcc or an hcp lattice with lattice parameter 1. A potential $V \in C^2(0, \infty)$ is α-localized if $\lim_{r\to\infty} V(r) = 0$,

$$\begin{aligned} V(r) &\ge \frac{1}{\alpha}, \quad r \in [0, 1-\alpha], \\ V''(r) &\ge 1, \quad 1-\alpha < r < 1+\alpha, \\ V'(r) &> 0 \quad r > 1+\alpha, \\ |V''(r)| &\le \alpha r^{-9}, \quad r > t(\mathcal{L}) + 2\alpha, \end{aligned}$$

and

$$\min_{r>0} \sum_{y\in\mathcal{L}\setminus\{0\}} V(r\,|y|) = \sum_{y\in\mathcal{L}\setminus\{0\}} V(|y|) = -12,$$

where $t(\mathcal{L})$ is the distance of third-nearest neighbors, $t(\mathcal{L}_{\rm fcc}) = \sqrt{3}$, $t(\mathcal{L}_{\rm hcp}) = \sqrt{8/3}$.

Theorem. Let $\mathcal{L} \subset \mathbb{R}^3$ be either a fcc or an hcp lattice with lattice parameter 1. There exist $\alpha_0 > 0$ such that for all $0 < \alpha < \alpha_0$ and all α-localized potentials V with the properties $V(\sqrt{2}) = -1/10$, $V(t(\mathcal{L})) = -1/50$ and

$$V'(r) + |V''(r)| < \alpha, \quad 1 + \alpha < r < \sqrt{2} + \alpha \text{ or } \sqrt{2} + 2\alpha < r < t(\mathcal{L}) + \alpha$$

the following holds.

(A) Ground state energy:

$$\lim_{n\to\infty} \min_{y\in\mathbb{R}^{3\times n}} E_n(\{y\}) = -6.$$

(B) Ground states: Let $A \subset \mathcal{L}$ be finite and $y : \mathcal{L} \to \mathbb{R}^3$ minimize

$$E(\{y\}) = \frac{1}{\#A} \sum_{\substack{i,j\in\mathcal{L} \\ \{i,j\}\cap A\neq\emptyset}} V(|y_i - y_j|)$$

subject to the constraint that $y_x = x$ for all $x \in \mathcal{L} \setminus A$. Then $y_i = i$ for all $i \in \mathcal{L}$, i.e. the minimizer is a perfect lattice.

The theorem is a significant extension of earlier results for two-dimensional systems [2]. The proof relies on rigidity estimates [1] and a new proof of the kissing problem by Oleg Musin [3].

References

[1] G. Friesecke, R. James and S. Müller, *A theorem on geometric rigidity and the derivation of nonlinear plate theory from three-dimensional elasticity*, Comm. Pure Appl. Math. **55** (2002), 169–204.

[2] F. Theil, *A proof of crystallization in two dimensions*, Comm. Math. Phys **262** (2006), 209–236.

[3] O.AMusin, *The kissing problem in three dimensions*, Discrete Comput. Geom. **35** (2006), no. 3, 375–384.

Reporter: Luca Mugnai

Participants

Virginia Agostiniani
SISSA
International School for Advanced Studies
Via Beirut n. 2-4
I-34014 Trieste

Prof. Giovanni Alberti
Dip. di Matematica "L.Tonelli"
Universita di Pisa
Largo Bruno Pontecorvo, 5
I-56127 Pisa

Prof. Dr. Hans Wilhelm Alt
Institut für Angewandte Mathematik
Universität Bonn
Wegelerstr. 6
53115 Bonn

Prof. Dr. Victor Berdichevsky
Department of Mechanical Eng.
2100 Engineering Building
Wayne State University
5050 Anthony Wayne Drive
Detroit , MI 48202-3902
USA

Prof. Dr. Davide Bigoni
Dipartimento di Ingegneria Meccanica e Strutturale
University of Trento
Via Mesiano, 77
I-38050 Trento

Prof. Dr. Luis L. Bonilla
Ciencias de Materiales
Campus Universidad Carlos III de Madrid
Avenida de la Universidad 30
E-28911 Leganes , Madrid

Prof. Dr. Guy Bouchitte
U.F.R. des Sc. et Techn.
Universite de Toulon et du Var
B.P. 132
F-83957 La Garde Cedex

Prof. Dr. Yann Brenier
Laboratoire J.-A. Dieudonne
UMR CNRS 6621
Universite de Nice Sophia-Antipolis
Parc Valrose
F-06108 Nice Cedex 2

Dr. Luca Cardamone
SISSA
International School for Advanced Studies
Via Beirut n. 2-4
I-34014 Trieste

Prof. Dr. Ana Maria Carpio
Departamento de Matematica Aplicada
Universidad Complutense de Madrid
E-28040 Madrid

Prof. Dr. Paolo Cermelli
Dipartimento di Matematica
Universita degli Studi di Torino
Via Carlo Alberto, 10
I-10123 Torino

Dr. Antonin Chambolle
Centre de Mathematiques Appliquees
Ecole Polytechnique
F-91128 Palaiseau Cedex

Prof. Dr. Antonio DeSimone
SISSA
International School for Advanced Studies
Via Beirut n. 2-4
I-34014 Trieste

Prof. Dr. Antonio Di Carlo
SMFM
Dept. of Studies on Structures
Universita Roma Tre
Via Corrado Segre, 6
I-00146 Roma

Dr. Nicolas Dirr
Department of Mathematical Sciences
University of Bath
Claverton Down
GB-Bath BA2 7AY

Dr. Patrick W. Dondl
Hausdorff Center for Mathematics
Institute for Applied Mathematics
Endenicher Allee 60
53115 Bonn

Prof. Dr. Marcelo Epstein
Dept. of Mechanical Engineering
University of Calgary
2500 University Drive N.W.
Calgary , AB T2N 1N4
CANADA

Livio Fedeli
SISSA
International School for Advanced Studies
Via Beirut n. 2-4
I-34014 Trieste

Prof. Dr. Adriana Garroni
Dipartimento di Matematica
"Guido Castelnuovo"
Universita di Roma "La Sapienza"
Piazzale Aldo Moro, 2
I-00185 Roma

Prof. Dr. Yury Grabovsky
Department of Mathematics
Temple University
Philadelphia , PA 19122
USA

Dr. Luca Heltai
SISSA
International School for Advanced Studies
Via Beirut n. 2-4
I-34014 Trieste

Prof. Dr. Hans Herrmann
ETH-Hönggerberg
Institut für Baustoffe
Schafmattstr. 6
CH-8093 Zürich

Prof. Dr. Jean-Francois Joanny
Institut Curie
Section Research, UMR 168
11, rue Pierre et Marie Curie
F-75248 Paris Cedex 05

Prof. Dr. Frank Jülicher
Max-Planck-Institut für Physik komplexer Systeme
Nöthnitzer Str. 38
01187 Dresden

Prof. Dr. Dr. Karsten Kruse
Fachbereich Theoretische Physik
Universität des Saarlandes
Postfach 151150
66041 Saarbrücken

Prof. Dr. Vladislav Kucher
Centre de Mathematiques
Ecole Polytechnique
C.N.R.S.
Plateau de Palaiseau
F-91128 Palaiseau Cedex

Prof. Dr. Sergei Kuksin
Centre de Mathematiques
Ecole Polytechnique
C.N.R.S.
Plateau de Palaiseau
F-91128 Palaiseau Cedex

Prof. Dr. Khanh Chau Le
Lehrstuhl für Allgemeine Mechanik
Ruhr-Universität Bochum
Fakultät für Bauingenieurwesen
Universitätsstr. 150
44801 Bochum

Dr. Marta Lewicka
School of Mathematics
University of Minnesota
127 Vincent Hall
206 Church Street S. E.
Minneapolis MN 55455-0436
USA

Prof. Dr. Stephan Luckhaus
Mathematisches Institut
Universität Leipzig
Johannisgasse 26
04103 Leipzig

Prof. Dr. Giuseppe Marrucci
Dipartimento di Ingegneria Chimica
Piazzale V. Tecchio 80
I-80125 Napoli

Prof. Dr. Alexander Mielke
Weierstraß-Institut für
Angewandte Analysis und Stochastik
im Forschungsverbund Berlin e.V.
Mohrenstr. 39
10117 Berlin

Prof. Dr. Ingo Müller
Institut für Verfahrenstechnik
FG Thermodynamik
Technische Universität Berlin
Fasanenstr. 90
10623 Berlin

Dr. Luca Mugnai
Max-Planck-Institut für Mathematik
in den Naturwissenschaften
Inselstr. 22 - 26
04103 Leipzig

Stefan Neukamm
Zentrum Mathematik
TU München
85747 Garching

Dr. Sebastien Neukirch
Institut Jean le Rond d'Alembert
Universite Pierre & Marie Curie
Paris VI, Case 162
4, place Jussieu
F-75252 Paris CEDEX 05

Prof. Dr. Stefano Olla
CEREMADE
Universite Paris Dauphine
Place du Marechal de Lattre de
Tassigny
F-75775 Paris Cedex 16

Prof. Dr. Michael Ortiz
Division of Engineering and
Applied Sciences; MS 104-44
California Institute of Technology
Pasadena , CA 91125
USA

Dr. Mark A. Peletier
Department of Mathematics
Eindhoven University of Technology
P.O.Box 513
NL-5600 MB Eindhoven

Dr. Francisco-Jose Perez-Reche
Department of Chemistry
University of Cambridge
Lensfield Road
GB-Cambridge CB2 1EW

Pierre Recho
Laboratoire Mecanique des Solides
Ecole Polytechnique
F-91128 Palaiseau Cedex

Dr. Oguz Umut Salman
Laboratoire Mecanique des Solides
Ecole Polytechnique
F-91128 Palaiseau Cedex

Andre Schlichting
Max-Planck-Institut für Mathematik
in den Naturwissenschaften
Inselstr. 22 - 26
04103 Leipzig

Dr. Bernd Schmidt
Zentrum Mathematik
Technische Universität München
85747 Garching bei München

Dr. Florian Theil
Mathematics Institute
University of Warwick
Zeeman Building
GB-Coventry CV4 7AL

Prof. Dr. Lev Truskinovsky
Laboratoire de Mecanique des
Solides
UMR-CNRS 7649
Ecole Polytechnique
F-91128 Palaiseau Cedex

Prof. Dr. Anna Vainchtein
Department of Mathematics
University of Pittsburgh
301 Thackery Hall
Pittsburgh , PA 15260
USA

Jens Wohlgemuth
Max-Planck-Institut für Mathematik
in den Naturwissenschaften
Inselstr. 22 - 26
04103 Leipzig

Dr. Giovanni Zanzotto
Dipartimento di Metodi e Modelli
Matematici
Universita di Padova
Via Trieste, 63
I-35121 Padova